



## **Monitoring oil contamination in vegetated areas with optical remote sensing: A comprehensive review**

Guillaume Lassalle, Sophie Fabre, Anthony Credo, Dominique Dubucq, Arnaud Elger

### **► To cite this version:**

Guillaume Lassalle, Sophie Fabre, Anthony Credo, Dominique Dubucq, Arnaud Elger. Monitoring oil contamination in vegetated areas with optical remote sensing: A comprehensive review. *Journal of Hazardous Materials*, 2020, 393, pp.122427. <10.1016/j.jhazmat.2020.122427>. <hal-02981700>

**HAL Id: hal-02981700**

**<https://hal.science/hal-02981700v1>**

Submitted on 28 Oct 2020

**HAL** is a multi-disciplinary open access archive for the deposit and dissemination of scientific research documents, whether they are published or not. The documents may come from teaching and research institutions in France or abroad, or from public or private research centers.

L'archive ouverte pluridisciplinaire **HAL**, est destinée au dépôt et à la diffusion de documents scientifiques de niveau recherche, publiés ou non, émanant des établissements d'enseignement et de recherche français ou étrangers, des laboratoires publics ou privés.



HAL Authorization

# Monitoring oil contamination in vegetated areas with optical remote sensing: a comprehensive review

*Guillaume Lassalle<sup>a, b, c, \*</sup>, Sophie Fabre<sup>a</sup>, Anthony Credo<sup>b</sup>, Dominique Dubucq<sup>c</sup>, Arnaud Elger<sup>d</sup>*

## AUTHOR ADDRESS

<sup>a</sup> Office National d'Études et de Recherches Aérospatiales (ONERA), Toulouse, France

<sup>b</sup> TOTAL S.A., Pôle d'Études et de Recherches de Lacq, Lacq, France

<sup>c</sup> EcoLab, Université de Toulouse, CNRS, INPT, UPS, Toulouse, France

<sup>d</sup> TOTAL S.A., Centre Scientifique et Technique Jean-Féger, Pau, France

\*Corresponding author: Guillaume Lassalle, Office National d'Études et de Recherches  
Aérospatiales, 2 Avenue Edouard Belin, 31055 Toulouse, France; E-mail:  
guillaumelassalle.pro@gmail.com

Keywords: remote sensing, reflectance spectroscopy, soil contamination, Total Petroleum  
Hydrocarbons, vegetation optical properties

## 15 ABSTRACT

16 The monitoring of soil contamination deriving from oil and gas industry remains difficult in  
17 vegetated areas. Over the last decade, optical remote sensing has proved helpful for this purpose.  
18 By tracking alterations in vegetation biochemistry through its optical properties, multi- and  
19 hyperspectral remote sensing allow detecting and quantifying crude oil and petroleum products  
20 leaked following accidental leakages or bad cessation practices. Recent advances in this field  
21 have led to the development of various methods that can be applied either in the field using  
22 portable spectroradiometers or at large scale on airborne and satellite images. Experiments  
23 carried out under controlled conditions have largely contributed to identifying the most important  
24 factors influencing the detection of oil (plant species, mixture composition, etc.). In a perspective  
25 of operational use, an important effort is still required to make optical remote sensing a reliable  
26 tool for oil and gas companies. The current methods used on imagery should extend their scope  
27 to a wide range of contexts and their application to upcoming satellite-embedded hyperspectral  
28 sensors should be considered in future studies.

## 29 MAIN ABBREVIATIONS

30 HM: Heavy Metal  
31 LAD: Lead Angle Distribution  
32 LAI: Leaf Area Index  
33 LCC: Leaf Chlorophyll Content  
34 LWC: Leaf Water Content  
35 NIR: Near-Infrared  
36 REP: Red-Edge Position  
37 RTM: Radiative Transfer Model

- 38 SWIR: Short-Wave Infrared
- 39 TPH: Total Petroleum Hydrocarbons
- 40 UAV: Unmanned Aerial Vehicle
- 41 UV: Ultraviolet
- 42 VI: Vegetation Indices
- 43 VIS: Visible

## TABLE OF CONTENTS

1. Introduction .....	4
2. Vegetation optical properties in the reflective domain (400 – 2500 nm) .....	9
2.1. Influence of leaf pigments in the visible region (400 – 750 nm) .....	10
2.2. Influence of leaf anatomy in the near-infrared region (750 – 1300 nm) .....	13
2.3. Influence of leaf water and dry matter contents in the near-infrared (750 – 1300 nm) and short-wave infrared (1300 – 2500 nm) regions .....	15
3. Effects of crude oil and petroleum products on vegetation health .....	17
3.1. Composition of crude oil and petroleum products .....	17
3.2. Effects on soil properties and on plant roots .....	19
3.3. Effects on plant biochemical and biophysical parameters .....	21
3.4. Sources of variability .....	23
4. Detection of crude oil and petroleum products using vegetation optical properties .....	27
4.1. Effects of crude oil and petroleum products on vegetation reflectance .....	27
4.2. Methods developed for detecting crude oil and petroleum products under controlled and field conditions .....	33
5. Application in contamination monitoring using airborne and satellite imagery .....	37
5.1. Synthesis based on previous studies .....	37
5.2. Perspectives toward operational applications in oil and gas industry .....	42
6. Conclusion .....	45

## 1. Introduction

Oil and gas industry currently holds a key role in the global energy mix [1–3]. Since the beginning of the 20<sup>th</sup> century, crude oil supply has continuously increased to satisfy a growing demand, reaching over 35 billion barrels (Gb) produced in 2017 [4–6]. Although a global peak of production – followed by a decline – is expected in the future, its timing remains largely unprecise as it depends on several factors, such as reserve estimates, and on the scenario that will frame the energy mix [7–10]. According to the International Energy Agency, oil production will become 8 million barrels per day greater in 2040 than today under the New Policy Scenario, which considers current government goals and policies. However, the increase of oil production

[11] goes together with a greater exposure of ecosystems to contamination, which remains a global ecological issue.

Once extracted from oil fields, crude oil is then refined to petroleum products [12–14]. At every step of the production process, oil spills and leakages may contaminate the soil and affect ecosystems. They result from facility failures, bad practices and storm events (Figure 1a-g). For example, extraction wells, pipelines, refineries and mud pits are common sources of contaminant leaked in the environment [15–20]. This includes crude oil, petroleum products, wastewaters and oil sludge [21–23]. All these contaminants cause severe ecological disturbances, such as landscape fragmentation and habitat loss or alteration, and affect human health [24–27]. Therefore, fast-detection is needed for assessing contamination and limiting its impacts. Lots of techniques have been developed for this purpose in response to major offshore oil spills [28]. However, the onshore domain – which stands for 70% of the global oil supply [29] – did not receive the same attention. Main advances have been achieved in pipeline leak detection, one of the most important source of oil contaminants in the environment [30–33]. Conversely, only little improvements have been made in assessing soil contamination deriving from extraction and refining activities or bad cessation management. Such operations are often made by field operators and do not guarantee an early detection of released contaminants, especially when it implies low and continuous quantities. They are time-consuming and lead to heavy ecological consequences when the contamination is not detected at early stage. Among promising alternatives, remote sensing could achieve fast detection of oil at large scale, fulfilling the needs of oil and gas companies. Encouraging perspectives of operational applications have emerged in this field, thanks to a growing interest over the last decades.



Figure 1. Principal sources of environmental contamination caused by oil activities. (a) Oil sludge pit [34], (b-c) vegetation and soil contaminated by crude oil leakage near a refining facility [35], (d) pipeline leakage [36], (e) crop contamination resulting from oil well blow out [37], (f) oil leakage from damaged storage tank following a storm [38] and (g) contaminated wastewater near a production site [39].

Active and passive remote sensing provide information about the composition of surfaces at large scale, by analyzing their radiometric properties in various domains of the electromagnetic spectrum [40,41]. Applications in onshore oil industry mainly rely on passive optical remote sensing, which exploits the [400:2500] nm reflective domain [42]. However, the real interest given to remote sensing by oil and gas companies started a few decades ago, with the emergence of passive hyperspectral sensors (Figure 2) [43]. Hyperspectral sensors provide reflectance data over multiple and contiguous wavelengths of the optical reflective domain [41]. They give access to the spectral signature of surfaces (*e.g.* waterbodies, soils, vegetation), which helps determining their composition (Figure 2). Hyperspectral imaging sensors include drone-/UAV-, airborne- and satellite-embedded sensors [44]. Some of them provide high to very high spatial resolution

images (metric to centimetric), making possible to detect small targets. In complement, field portable spectroradiometers are usually used for collecting point reflectance data under controlled conditions or in the field [45]. The use of hyperspectral sensors for detecting apparent oil usually relies on exploiting the optical properties of petroleum hydrocarbons. For example, recent attempts succeeded in detecting contamination around industrial facilities using hyperspectral airborne and satellite imagery, by exploiting the spectral signature of soils [35,46]. From an operational point of view, hyperspectral imagery could thus provide a rapid diagnosis of oil-contaminated surfaces at large scale, but serious limits still compromise its use in vegetated regions.

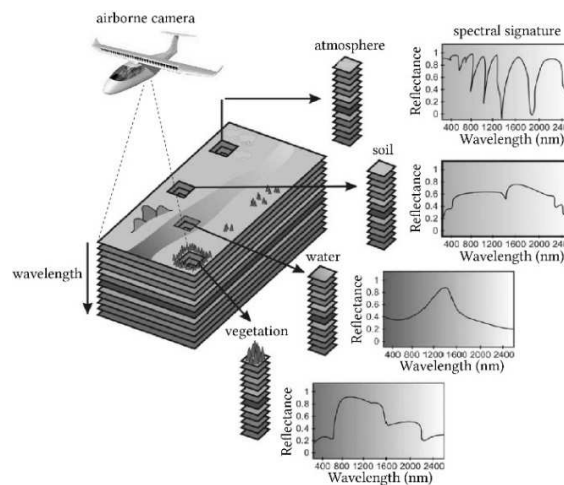


Figure 2. Principle of passive hyperspectral imagery (adapted from [47]). This technology provides the reflectance of surfaces over a continuous spectrum in the optical reflective domain (*i.e.* the spectral signature).



On sites covered by dense vegetation, optical remote sensing remains ineffective for detecting oil seepages and leakages directly, because light penetration is strongly limited by the foliage and the spectral signature of soils is thus not accessible. The only information about soil composition can be provided indirectly by vegetation through its optical properties [48–50]. This can be achieved because vegetation reflectance is closely linked to its biophysical and biochemical parameters (*e.g.* pigments), which are good indicators of environmental – especially stressful – conditions [51–53]. Consequently, unfavorable growing conditions in soils result in modifications of vegetation health and optical properties that can be tracked using hyperspectral remote sensing [23,54,55]. Therefore, since crude oil and petroleum products affect vegetation health, they can be detected and quantified indirectly using optical imagery [56–59]. To achieve this, several conditions must be fulfilled: (1) The contamination must affect the biophysical and biochemical parameters of vegetation, (2) alterations in these parameters must modify the spectral signature of vegetation and (3) the specifications of imaging sensors (*e.g.* the spatial and spectral resolutions) must make it possible to track these alterations. This implies good knowledge about the parameters of vegetation influencing its reflectance, as well as their response to oil contamination. Recent studies carried out under controlled and natural conditions have highlighted the need to develop methods specifically dedicated to this purpose, as well as the current pitfalls and limits to overcome [50,54,55,58]. Hence, an important effort still remains to make hyperspectral remote sensing an operational tool for monitoring oil contamination. Yet, no review has been proposed in that field. Previous review focused either on heavy metals contamination deriving from agriculture and mining [60,61] or on *soil contamination* in general [62,63]. However, recent studies emphasized that crude oil and petroleum products cannot be

151 treated in the same way as other contaminants when assessing soil contamination from vegetation  
152 reflectance. Hence, they must be addressed separately.

153 The present review is intended to provide a comprehensive state-of-the-art of advances and  
154 challenges in the use of optical remote sensing for monitoring oil contamination in vegetated  
155 areas. It is addressed to non-specialists from a wide range of disciplines. This review is  
156 organized in accordance to the three points listed above. A first section summarizes the optical  
157 properties of vegetation in the reflective domain. Then, an overview of the effects induced by oil  
158 contamination on vegetation health is proposed. These two sections introduce key notions for  
159 non-specialists. Finally, the following sections go further into details of the topic. They focus on  
160 the consequences on these effects on vegetation reflectance and the methods developed to detect  
161 them under controlled and field conditions and using airborne and future satellite imagery.

## 163 2. Vegetation optical properties in the reflective domain (400 – 2500 nm)

164 Over the last 30 years, vegetation health assessment sparked an extensive attention by the  
165 remote sensing community. Then, the development of airborne- and satellite-embedded optical  
166 sensors opened the way to various applications in agriculture and ecology, thanks to a better  
167 comprehension of vegetation optical properties. The use of field portable spectroradiometer  
168 helped achieving this by providing reflectance data acquired at leaf or canopy scales. In the  
169 reflective domain, vegetation optical properties are driven by biophysical and biochemical  
170 parameters. They provide a singular shape to the spectral signature of healthy green vegetation,  
171 characterized by a peak of reflectance in the visible (VIS, 400 – 750 nm), a plateau in the near-  
172 infrared (NIR, 750-1300 nm) and two marked peaks in the short-wave-infrared (SWIR, 1300 –

2500 nm) (Figure 3). Leaf pigment and water contents and anatomy are the main parameters involved.

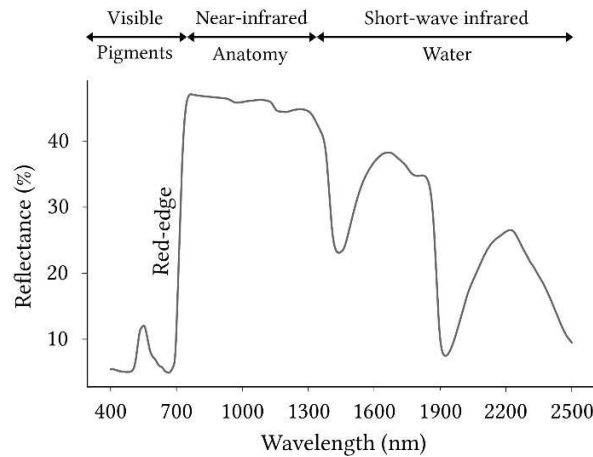


Figure 3. Typical spectral signature of healthy green leaf and most influential parameters in the different spectral regions.

## 2.1. Influence of leaf pigments in the visible region (400 – 750 nm)

A large diversity of pigments is present in plants [64–66]. Pigments are essential to the development of vegetation, because of their implications in photochemical reactions. They absorb light at various wavelengths in the ultraviolet (UV) and VIS regions, depending on their chemical properties. Consequently, the spectral signature of vegetation is strongly linked to leaf pigment content between 400 and 750 nm [64,67,68]. This makes possible to track changes in pigments using multi- and hyperspectral sensors.

Chlorophylls a and b are the main pigments present in leaves. They are good indicators of vegetation health [69–71], making them largely studied in remote sensing [72–74]. Chlorophyll concentration usually ranges from 0 to 80  $\mu\text{g}\cdot\text{cm}^{-2}$  in crops [75], of which only 20% are represented by chlorophyll b in healthy green leaves [76]. These pigments show two light

absorption peaks at 440-450 (blue) and 650-670 nm (red) [77,78]. Due to their important concentration in leaves, chlorophylls have a strong influence on the spectral signature, so they are likely to hide the effects of other pigments sharing common absorption wavelengths. More precisely, the weak light absorption of chlorophylls around 550 (green) and 700 nm (red-edge) results in high correlation with leaf reflectance in these regions [67,79]. Hence, remote sensing mostly exploits these wavelengths to quantify leaf chlorophyll content (LCC) [74]. A large diversity of approaches have been developed for tracking changes in LCC, such as simple or normalized reflectance ratios (vegetation indices (VI)) and Radiative Transfer Models (RTM) [52,64]. These approaches gave particular attention to the inflexion point of reflectance in the red-edge region – named the *Red-Edge Position* (REP), which is sensitive to little changes in LCC (Figure 3) [73,80,81].

Carotenoids are the other photosynthetic pigments found in plants [82]. They can be distinguished in two categories: carotenes and xanthophylls, which absorb light mainly in the blue region (400 – 500 nm). This common feature with chlorophylls explains their masking in healthy leaves, as their concentration rarely exceeds  $25 \mu\text{g.cm}^{-2}$  [75]. They are usually less influential on the spectral signature in the VIS and thus more difficult to quantify by remote sensing. However, the chlorophyll breakdown observed during leaf senescence increases the carotenoid-chlorophyll ratio [76,83]. Consequently, leaf reflectance rises between 500 and 750 nm (green – red), so carotenoids become more easily quantifiable (Figure 4).

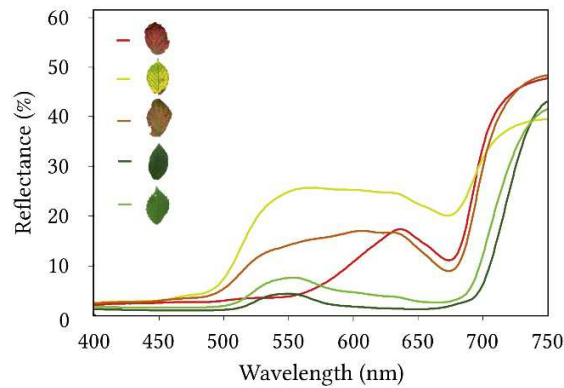


Figure 4. Spectral signatures of *Rubus fruticosus* L. in the visible region across different seasonal stages (unpublished data).

Frequently described as accessory pigments, carotenoids ensure essential photoprotective functions in plants [84,85]. They prevent leaf tissues from harmful effects of reactive oxygen species and photochemical stress that occur when absorbed light exceeds the photosynthetic capacity of leaves [82,83]. Therefore, the quantification of leaf carotenoid content is of great importance for monitoring vegetation health. Several VI have been designed for this purpose, such as the Photochemical Reflectance Index (PRI) [86,87]. The PRI exploits reflectance at 531 and 570 nm to track the epoxidation state of the xanthophyll cycle and can be used for assessing variations of photosynthetic activity across seasons [88,89].

Leaves also contain non-photosynthetic pigments that are responsible for color changes in autumn. Several plants turn red during senescence, because of the accumulation of anthocyanins in vacuoles. Anthocyanins are water-soluble flavonoids that absorb light in the ultraviolet (UV, 250 – 350 nm) and green (500 – 560 nm) regions [90,91]. They ensure a photoprotective function through UV screening, making them relevant indicators of vegetation health [92,93]. Other compounds such as tannins are also found in leaves, but their influence on leaf optical

properties is restricted to the late senescence – or pre-abscission – period [83]. They are responsible for the browning of leaves.

## 2.2. Influence of leaf anatomy in the near-infrared region (750 – 1300 nm)

As pigments do in the VIS, leaf anatomy drives reflectance in the NIR region [53,94]. Leaves of Angiosperms are formed by successive cellular layers structured in parenchyma – also called mesophyll – and protected by a cuticle and an epidermis on abaxial (lower) and adaxial (upper) faces. This anatomy is at the origin of the plateau observed on leaf spectral signature in the NIR (Figure 3), ranging from 30 to 80% reflectance [53,95,96]. The upper cuticle and epidermis are the first barriers to the penetration of light. Incident light follows diffuse and specular reflection at leaf surface, but most radiations go through it and are transmitted to lower layers [97,98].

The internal anatomy of leaves greatly contribute to their optical properties in the NIR, but differs between mono- and dicotyledonous species [95,99,100]. In dicotyledonous leaves, cells are typically arranged in two distinct parenchyma. The upper one – known as palisade parenchyma – is made of well-structured elongated cells with high chloroplast concentration. Intercellular spaces are almost absent from this layer so light scattering remains limited. Conversely, the lower – spongy – parenchyma is characterized by irregularly-shaped and spaced cells with low chloroplast content. The spongy parenchyma has an important function in leaves, as it sends back a fraction of incident light to the palisade parenchyma, thus increasing the photosynthetic activity [101]. In monocotyledonous leaves, parenchyma are undifferentiated. Cells form a unique layer similar to the spongy parenchyma of dicotyledonous leaves, although this one is more compact so intercellular spaces are reduced. Several studies showed that the cuticle and parenchyma thickness, the proportion of intercellular spaces and the arrangement of

chloroplasts greatly affect leaf reflectance in the NIR [53,94,95,102]. Leaf anatomy substantially varies among species, partly as a result of phylogeny and adaptation to light conditions [103–105]. Additional factors also influence leaf anatomy and NIR reflectance, such as nutrient and water availability or soil contamination.

While the anatomy of leaves determines their reflectance in the NIR, other biophysical parameters prevail when measuring reflectance at canopy scale. The Leaf Area Index (LAI) and the Leaf Angle Distribution (LAD) are the most influential ones [51,101,106]. Canopy reflectance is positively correlated to LAI in the NIR, because the influence of bare soil is reduced in this region as LAI increases (Figure 5) [107]. However, the reflectance reaches a plateau above very high LAI values ( $>6$ ) [101]. LAD characterizes canopy architecture, *i.e.* the angular orientation of leaves. de Wit [108] proposed to classify species in the following six LAD types: Planophile, plagiophile, erectophile, extremophile, spherical and uniform. As leaf orientation is moving away from zero degrees (toward planophile LAD), canopy reflectance decreases in the NIR [51].

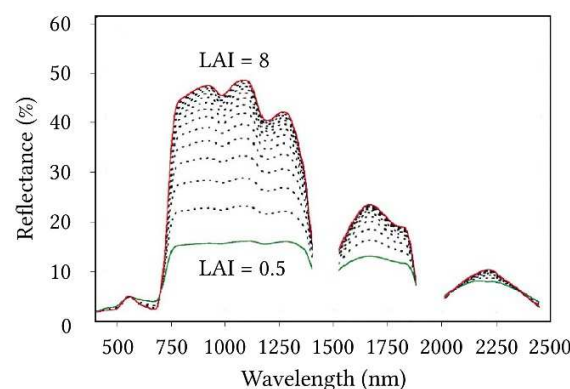


Figure 5. Influence of the Leaf Area Index (LAI) on canopy reflectance [51].

Because of its relationship with vegetation biophysical parameters, reflectance in the NIR can be used to describe leaf anatomy, canopy architecture and ground cover [53,109]. These parameters have in common to be directly or indirectly influenced by vegetation water status [96,110,111]. Water availability is a key parameter for understanding vegetation optical properties, as it drives many physiological mechanisms.

### 2.3. Influence of leaf water and dry matter contents in the near-infrared (750 – 1300 nm) and short-wave infrared (1300 – 2500 nm) regions

Vegetation optical properties are directly influenced by water contained in leaves, which absorbs light around 970, 1200, 1450, 1950 and 2450 nm [112–114]. These features are easily observed on the spectral signature of healthy plants and are affected by changes in leaf water content (Figure 6) [96]. Hence, they are reliable indicators of vegetation water status [115]. In addition, water is likely to affect reflectance indirectly in other spectral regions, as it is involved in many physiological mechanisms in plants, such as photosynthesis and leaf turgor. This is particularly marked for plants undergoing water-deficit stress [57,116]. Changes in leaf turgor and tissue destructuring induced by insufficient water uptake greatly affect light scattering and thus leaf reflectance in the whole NIR region [96]. These effects are also observed at canopy scale, as plant LAI and LAD are also modified by water-deficit stress [117].



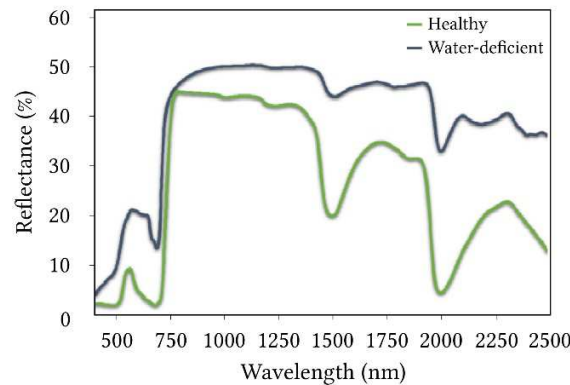


Figure 6. Spectral signatures of healthy and water-deficient plants.

Several studies demonstrated the effectiveness of the NIR and SWIR reflectance to assess vegetation water status by estimating Leaf Water Content (LWC) or Equivalent Water Thickness (EWT) [112,113,115]. VI and RTM have been widely used for this purpose [118–121]. Although water absorption bands previously cited may be appropriate [112,113], their utilization remains limited in airborne or satellite imagery, because of important noise due to atmospheric effects of water vapor. This limit can be however overcome by exploiting other water-dependent and atmospherically-resistant wavelengths in the NIR and SWIR regions [121–123].

As described in this section, vegetation optical properties are strongly linked in the NIR and SWIR regions, because of direct and indirect influence of water. According to Ceccato *et al.* [119], water stands for approximately 55 to 75% of healthy leaf fresh weight for temperate species. More than two thirds of the remaining part come from hemicelluloses, celluloses, lignins and proteins, which are often grouped in the “dry matter” term [124,125]. Celluloses are the most abundant organic compounds on earth and are found in all plants. Hemicelluloses and lignins are mostly represented in woody species [126,127]. These biochemical parameters share common light absorption features in the NIR and SWIR regions, at 1200, 1450 – 1490, 1540, 1760, 2100 and 2340 nm [128]. Proteins show quite different light absorption features, located at 1510 –

1520, 1730, 1980, 2060, 2165 – 2180 and 2300 nm. All these parameters remain difficult to estimate from vegetation reflectance, because their influence on reflectance in the NIR and SWIR regions is limited in comparison to water [124,128]. They become however more influential in dry leaves. Few VI have been designed for retrieving celluloses and lignins content in leaves or decomposing litter [129,130].

As outlined in this section, the biophysical and biochemical parameters driving vegetation optical properties differ according to the spectral region (VIS, NIR and SWIR). Modifications in these parameters are expressed as changes in the reflectance of leaves and canopies. This makes possible to detect oil-induced alterations in vegetation health using multi- and hyperspectral remote sensing. This purpose however requires identifying the most suitable (*i.e.* oil-sensitive) spectral regions. A good comprehension of the effects induced by crude oil and petroleum products on vegetation is mandatory for achieving it. These effects are described in the following section.

### 3. Effects of crude oil and petroleum products on vegetation health

Crude oil and petroleum products leaked from industrial facilities are likely to affect vegetation health and optical properties. Their particular nature and composition are greatly responsible for these effects.

#### 3.1. Composition of crude oil and petroleum products

Crude oil refers to oil in its natural and extractible form, *i.e.* oil stored in geological formation and brought to the surface [12]. Petroleum products result from the refining of crude oil. They include fuels (diesel, gasoline, kerosene), lubricant, waxes and miscellaneous products used in

various domains (*e.g.* transportation and industry) [131]. The term oil refers both to crude oil and petroleum products. Wastewaters and oil sludge are produced during the refining process [21,22]. Both crude oil and petroleum products are mixtures of volatile to dense hydrocarbons (called *Petroleum hydrocarbons*), heavy metals (HM, also termed *Trace Metal Elements*) and oxygen, sulfur and nitrogen compounds in various proportions [132–134]. Petroleum hydrocarbons include Mono- and Polycyclic Aromatic Hydrocarbons (BTEX and PAH, respectively), and saturated (alkanes or paraffins) and unsaturated (alkenes and alkynes) hydrocarbons [131]. *Total Petroleum Hydrocarbons* (TPH) is a generic term that encompasses all these compounds. Depending on the length of their carbon chain, petroleum hydrocarbons are refined to different petroleum products [135,136]. An illustration is given in Figure 7.

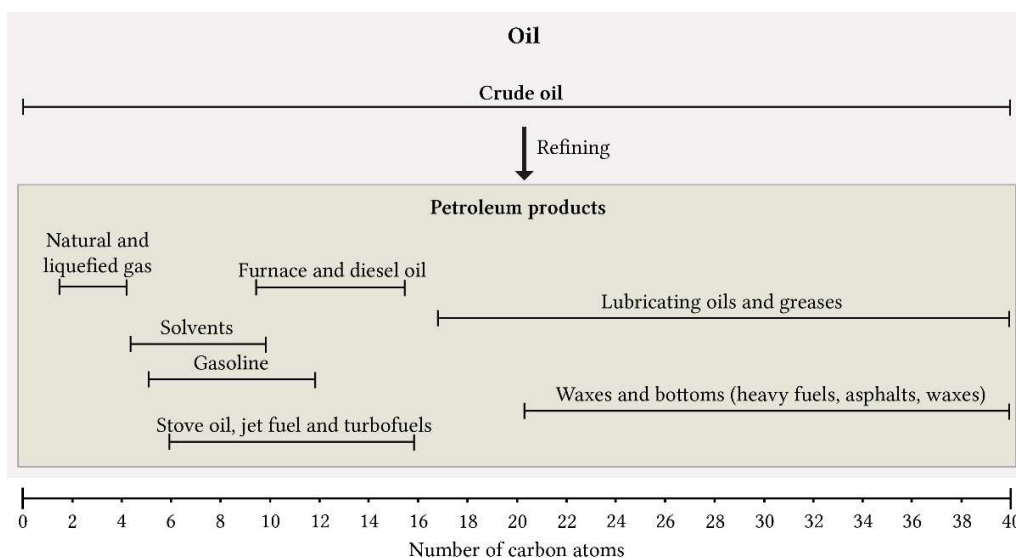


Figure 7. Crude oil and petroleum products according to petroleum carbon ranges (reproduced from [136]).

The composition of crude oil and petroleum products gives them a high toxicity towards vegetation [137]. When considered separately, each hydrocarbon and HM type is likely to affect

vegetation health [138]. Since they are in mixture, it remains difficult to identify which of these compounds are responsible for the observed response. In addition, interactions can occur among hydrocarbons and HM and result in synergistic or antagonist effects on vegetation [57]. However, the influence of mixture composition is still misunderstood. Different mixtures such as crude oil, diesel or gasoline, lead to different responses of vegetation [57,58,139]. These responses result from indirect effects caused by modifications of soil physico-chemical and biological properties, and from direct effects through contact with plant and assimilation in tissues [140,141]. Both occur at root level and lead to anatomical and biochemical changes in leaves, so these direct and indirect effects remain difficult to differentiate [142–144]. They are described jointly here.

### 3.2. Effects on soil properties and on plant roots

The phytotoxicity of petroleum hydrocarbons and HM has been subject to numerous studies. However, no review has been proposed – for terrestrial plants – in this field for almost 50 years [137]. Since then, few studies have focused on the effects of petroleum hydrocarbons and HM in mixture [56,145,146]. This topic has been addressed recently and provided a better comprehension of how vegetation is affected by oil leakages.

Because of their particular nature and composition, crude oil and petroleum products induce important modifications of soil physico-chemical and biological properties [134,147,148]. Consequently, they impose selective growing conditions to plants [55]. Soil water regime is one of the most impacted properties. Because of hydrocarbons, crude oil and petroleum products are in liquid – highly hydrophobic – form [131]. When found in soils, they occupy a fraction of porosity that becomes unavailable to water. In addition, by interacting with soil materials

(especially clay), oil forms a hydrophobic film at their surface, which forces water drainage toward deeper soil layers. These phenomena contribute to reducing the field capacity of soil and plant water supply [149–151]. It is amplified by HM, which affect soil water potential and water uptake by roots once transferred to the soil solution [152].

Petroleum hydrocarbons represent a considerable enrichment in organic material, leading to an increase of soil carbon content and carbon / nitrogen ratio (C/N) [134,151,153]. This stimulates the growth of microorganisms capable of degrading hydrocarbons, thus modifying organic matter mineralization cycles and reshaping microorganism communities [154–156]. The biodegradation of hydrocarbons is accompanied by an elevation of soil CO<sub>2</sub> concentration, especially in the presence of vegetation [157]. Some of the HM found in oil are essential to vegetation growth (*e.g.* Fe, Zn, Cu), but their occurrence at high concentrations along with other HM (*e.g.* Cd, Mg, Pb) also affect microorganisms [158]. They are not degradable and in the case of oil leakages, they concentrate in the first soil layers [159]. The nitrogen cycle is particularly impacted by carbon enrichment: the availability of inorganic nitrogen decreases so vegetation nitrogen status is highly altered [153]. Likewise, several studies revealed that petroleum hydrocarbons and HM reduce nutrient availability (P, K) and soil Cation Exchange Capacity (CEC) [150,151,160]. The latter is indeed closely linked to soil organic matter content, C/N ratio and pH; so many parameters affected by oil [132,134]. Through modifications of soil physico-chemical and biological properties, crude oil and petroleum products thus affect water and nutrient availability for plants [161]. These effects are called indirect effects. In addition, direct effects occur when oil is in contact with roots [162]. As they do with soil materials, petroleum hydrocarbons are able to coat plant roots by adsorbing at their surface. As well as HM, their assimilation inhibits root growth and causes a thickening of root epidermis, endodermis and

cortex, and a reduction of root hair diameter and density [140,152,163,164]. These anatomical changes heavily alter water and nutrient uptake capacities of plants. For some species, they are partly compensated by a higher allocation of resources to roots.

As soon as water or nutrient supply is no longer sufficient to ensure essential physiological functions, stressful conditions arise so plant undergoes anatomical and biochemical modifications that affect its reflectance. These effects are amplified by the accumulation of certain hydrocarbons and HMs in leaves [138,141,142].

### 3.3. Effects on plant biochemical and biophysical parameters

The biophysical and biochemical parameters affected by exposure to crude oil and petroleum products are involved in vegetation optical properties. A review of these effects is proposed in Table 1. The alteration of leaf pigment content is the most frequently described response of plant to crude oil and petroleum products [58,142,165]. This alteration is induced by that of plant water and nitrogen status described above [149]. It can be visually observed through symptoms of leaf discoloration, which vary among species and according to mixture composition [57,59,163] (Figure 8a-d). The discoloration is caused by a reduction of LCC and indicates a decrease in photosynthetic activity [139]. This response is very common for water-deficient plants [37,111]. Although they are naturally present at lower concentrations in leaves, carotenoids and anthocyanins are also affected [58]. HM accumulation amplifies this effect [152,166].

Alterations of biophysical parameters can be observed at different scales. At leaf scale, they are expressed as a reduction in the number and size of cells and an increase of intercellular spaces in parenchyma [142,144]. The accumulation of certain hydrocarbons and HMs –

412 especially Cd and Mg – also causes tissue destructuring [137,138]. Consequently, important  
413 modifications of leaf spectral signature are expected in the NIR region. At canopy scale, water  
414 and nutrient deficiency leads to a limited development (*i.e.* a reduction of leaf and stem length  
415 and density), reducing aboveground biomass and LAI. In addition, changes in leaf anatomy and  
416 water content affect plant habit and consequently LAD.

417

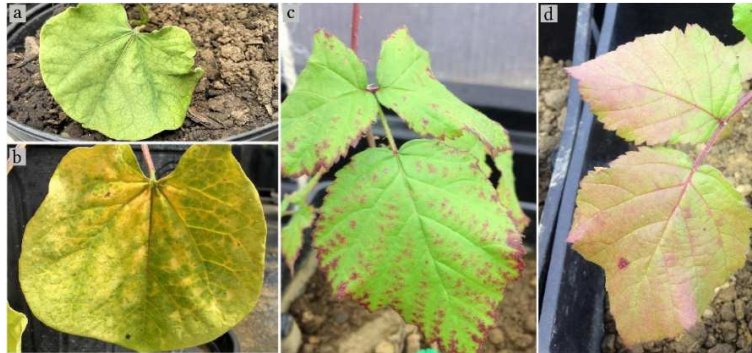


Figure 8. Visible stress symptoms commonly observed on leaves under exposure to crude oil and petroleum products. These symptoms are associated to alteration in pigment content. (a-b) *Canavalia ensiformis* (L.) DC grown on diesel-contaminated soil [163]. (c-d) *Rubus fruticosus* L. grown on (c) mud pit- and (d) crude oil-contaminated soils [57].

### 3.4. Sources of variability

The severity of the effects described in section 3.3 highly varies according to the context as described in Table 1, because these effects are influenced by many factors. The sensitivity of the species is a determining one [49,167,168]. Since all species do not share similar ecological requirements, their tolerance to stressful conditions differs. Consequently, a decrease in soil water and nutrient availability caused by crude oil and petroleum products will not affect all species in the same way [169]. Moreover, some species are capable of detoxifying hydrocarbons and HMs accumulated in leaves through mechanisms of sequestration, transportation and excretion [145,170]. This prevents biochemical alterations and tissue destructuring. Few species are even stimulated by the enrichment of soil organic matter provided by crude oil and petroleum products, but this response remains uncommon [171,172]. This variability in species' sensitivity has strong implications under natural conditions. For example, only few species are established around natural oil seepages [55]. Their presence is explained by a high tolerance to chronic crude



oil exposure, so these species undergo no or little alterations. Mud pits contaminated by oil production residues (*e.g.* oil sludge) are similar cases [16,49,56,57,161]. Conversely, crude oil and petroleum products leaked from drilling well, storage tank and pipeline leakages consist in a rapid exposure of oil-intolerant species. In those conditions, severe alterations and sometimes plant death are observed [26,58,165].

Petroleum hydrocarbon and HM availability for plants strongly varies according to their chemical properties. For example, low-carbon PAHs and As are easily accumulated in leaves [138]. Therefore, mixture composition influences plant response, so different crude oils or petroleum products (*e.g.* diesel, gasoline) do not affect leaf biophysical and biochemical parameters of a single species in the same extent [57,137,141]. Apart from mixture composition, these effects are also conditioned by the level and time of exposure to oil [58,149,168]. More precisely, the amplitude of pigment and water content alteration in leaves is positively correlated to the overall TPH concentration [49]. Above a threshold concentration that depends on species' sensitivity (generally in  $\text{g.kg}^{-1}$ ), plant death can be observed after only few days [142,167]. In contrast, several weeks of exposure might be required to induce biophysical and biochemical alterations at low concentrations ( $\mu\text{g}$  to  $\text{mg.kg}^{-1}$ ) [163,172].

Although the effects of petroleum hydrocarbons and HM mixtures on vegetation are well documented in the literature, they cannot be generalized to all contexts of oil leakages because their severity depends on many factors. Species' sensitivity, mixture composition and concentration and exposure time have been identified as the most influential ones. These factors have critical implications in remote sensing, since they determine the amplitude of reflectance changes in vegetation and thus hydrocarbon detectability using airborne and satellite-embedded sensors.

Table 1. Effects induced by crude oil and petroleum products on vegetation biophysical and biochemical parameters. (↑ and ↓ denotes increase and decrease in the measured parameter, respectively; \* indicates dose-dependent effects; n.a.: not available or not measured.)

Species	Crude oil Petroleum product	TPH	Total time of exposure	Anatomy / Development	Pigments / Photosynthesis	Water status	Ref.
<i>Ailanthus altissima</i> Mill.	Oil sludge	10-40%	240 days	↓ Shoot length and biomass*	↓ Photosynthesis*	↓ Stomatal conductance* ↓ Leaf transpiration*	[173]
<i>Allophylus edulis</i>	Crude oil	13.65 g.kg <sup>-1</sup>	30-60 days	↑ Shoot length and biomass unchanged	n.a.	n.a.	[162]
<i>Amorpha fruticosa</i>	Crude oil	5-20 g.kg <sup>-1</sup>	6 months	↓ Shoot biomass*	↓ Leaf chlorophyll content*	↓ Leaf water content ↓ Stomatal conductance and transpiration rate*	[174]
<i>Canavalia ensiformis</i>	Diesel	22,219 mg.kg <sup>-1</sup>	30 days	↓ Palisade and spongy parenchyma thickness ↓ Stem and leaf length and biomass	Leaf discoloration and necrosis ↓ Leaf chlorophyll content ↓ Leaf carotenoid content	n.a.	[163]
<i>Capsicum annum</i>	Lubricating oil	1-5%	84 days	↓ Shoot length* ↓ Leaf area*	n.a.	n.a.	[167]
<i>Cedrela odorata</i>	Crude oil	18-47.10 g.kg <sup>-1</sup>	245 days	↓ Shoot length and biomass	n.a.	n.a.	[168]
<i>Corchorus olitorius</i>	Engine oil	0.2-3%	6 weeks	↓ Shoot length* ↓ Leaf area*	↓ Leaf chlorophyll content*	↓ Leaf water content*	[175]
<i>Cyperus brevifolius</i>	Crude oil	10-50 g.kg <sup>-1</sup>	6 months	↑ Cuticle thickness* ↓ parenchymatous cell length and diameter* ↓ intercellular spaces length and diameter* ↓ Shoot biomass*	Light to very dark leaves ↓ Leaf chlorophyll content*	n.a.	[142]
<i>Deschampsia caespitosa</i>	Petroleum cokes	n.a.	3 months	↓ Shoot length	↓ Leaf chlorophyll content ↓ Leaf carotenoid content	↓ Transpiration rate and stomatal conductance	[176]
<i>Fraxinus rotundifolia</i> Mill.	Oil sludge	10-40%	240 days	↓ Shoot length and biomass*	↓ Photosynthesis*	↑ Stomatal conductance until day 80* ↓ Stomatal conductance after day 80* ↓ Leaf transpiration*	[173]
<i>Glycine hyspida</i>	Crude oil	1.3-3.1 g.kg <sup>-1</sup>	>6 months	↓ Shoot biomass*	n.a.	n.a.	[134]
	Crude oil (spill)	1.1-3.8 g.kg <sup>-1</sup>	>6 months	↓ Shoot biomass*	n.a.	n.a.	
	Drilling fluids	1.6-76.1 g.kg <sup>-1</sup>	>6 months	↓ Shoot biomass*	n.a.	n.a.	
<i>Haematoxylum campechianum</i>	Crude oil	18-47.10 g.kg <sup>-1</sup>	245 days	↓ Shoot length and biomass	n.a.	n.a.	[168]
<i>Hordeum vulgare</i>	Crude oil	1.3-3.1 g.kg <sup>-1</sup>	>6 months	↓ Shoot biomass	n.a.	n.a.	[134]
	Crude oil (spill)	1.1-3.8 g.kg <sup>-1</sup>	>6 months	Shoot biomass unchanged	n.a.	n.a.	
	Drilling fluids	1.6-76.1 g.kg <sup>-1</sup>	>6 months	↓ Shoot biomass*	n.a.	n.a.	
<i>Lycopersicon esculentum</i>	Lubricating oil	1-5%	84 days	↓ Shoot length* ↓ Leaf area*	n.a.	n.a.	[167]

Species	Crude oil Petroleum product	TPH	Total time of exposure	Anatomy / Development	Pigments / Photosynthesis	Water status	Ref.
<i>Medicago sativa</i>	Oil sludge	4-5%	9 weeks	↓ Shoot length and biomass unchanged	n.a.	n.a.	[161]
<i>Melia azedarach L.</i>	Oil sludge	10-40%	240 days	↓ Shoot length and biomass* ↓ Leaf area	↓ Photosynthesis*	↓ Stomatal conductance* ↓ Leaf transpiration*	[173]
<i>Phragmites australis</i>	Crude oil	2-12 g.kg <sup>-1</sup>	2 months	↓ Shoot biomass*	n.a.	n.a.	[153]
<i>Robinia pseudoacacia L.</i>	Oil sludge	10-40%	240 days	↓ Shoot length and biomass* ↓ Leaf area	↓ Photosynthesis	↓ Stomatal conductance	[173]
<i>Swietenia macrophyll</i>	Crude oil	18-47.10 g.kg <sup>-1</sup>	245 days	↓ Shoot length and biomass	n.a.	n.a.	[168]
<i>Tabebuia rosea</i>	Crude oil	18-47.10 g.kg <sup>-1</sup>	245 days	↓ Shoot length and biomass	n.a.	n.a.	[168]
<i>Terminalia catappa</i>	Crude oil (spill)	n.a	3 weeks	↑ Cuticle thickness ↑ Epidermal cell diameter ↑ Palisade and ↓ spongy parenchyma thickness	n.a.	n.a.	[144]
<i>Triticum aestivum</i>	Crude oil	1.3-3.1 g.kg <sup>-1</sup>	>6 months	↓ Shoot biomass	n.a.	n.a.	[134]
	Crude oil (spill)	1.1-3.8 g.kg <sup>-1</sup>	>6 months	↓ Shoot biomass*	n.a.	n.a.	
	Drilling fluids	1.6-76.1 g.kg <sup>-1</sup>	>6 months	↓ Shoot biomass*	n.a.	n.a.	
<i>Triticum aestivum</i>	Petroleum cokes	n.a	2 months	↓ Shoot length ↓ Leaf area	↓ Leaf chlorophyll content ↓ Leaf carotenoid content	↓ Transpiration rate and stomatal conductance	[176]
<i>Vicia faba</i>	Crude oil	1.56-50%	30 days	↓ Shoot biomass	↓ Leaf chlorophyll content Leaf carotenoid content unchanged	↓ Leaf water content	[177]
<i>Vicia faba</i>	Crude oil	9-18 g.kg <sup>-1</sup>	5 weeks	↓ Shoot length and biomass*	n.a.	n.a.	[141]
	Diesel	9-18 g.kg <sup>-1</sup>	5 weeks	↓ Shoot length and biomass*	n.a.	n.a.	
	Engine oil	9-18 g.kg <sup>-1</sup>	5 weeks	↓ Shoot length and biomass*	n.a.	n.a.	
<i>Zea mays</i>	Crude oil	0.28-0.66%	6 weeks	↓ Shoot biomass	↓ Leaf chlorophyll content	↓ Leaf water, osmotic and turgor potentials	[149]

#### 4. Detection of crude oil and petroleum products using vegetation optical properties

The previous introductory sections provided key elements to understand how the biophysical and biochemical parameters of vegetation drives its reflectance, and how these parameters are affected by oil contamination. It is therefore expected that these biophysical and biochemical alterations will modify the reflectance of vegetation, at leaf and plant scales, making possible to detect oil contamination indirectly. This section summarizes the modifications of vegetation reflectance induced by crude oil and petroleum products, and the existing methods developed to track these modifications, under controlled and field conditions.

Vegetation optical properties have been extensively used for tracking alterations in pigment or water content caused by biotic and abiotic factors [178–182]. Conversely, their exploitation in oil leakage detection has been initiated more recently [57,59,165]. Major progress has been made in this field by taking advantage of multi- and hyperspectral methods developed for assessing vegetation health in other contexts, such as crop and ecosystem monitoring. Some of these methods – especially VI and RTM – proved efficient for tracking oil-induced alterations in vegetation reflectance under controlled and field conditions, from spectroradiometer-acquired reflectance data [57,59,172,183].

##### 4.1. Effects of crude oil and petroleum products on vegetation reflectance

As described in section 3, crude oil and petroleum products affect the main biophysical and biochemical parameters driving vegetation optical properties. These effects result in modifications in the spectral signature at leaf and canopy scales, which have been studied under greenhouse or field conditions. They are summarized in Table 2. The VIS has been mostly exploited for tracking the effects of crude oil and petroleum products from the spectral signature

of vegetation, because of its strong link with pigments [59,139,165,183]. The alteration of chlorophyll content described in the previous section immediately leads to an increase of reflectance in this region, at leaf and canopy scales (Figure 9) [57,58]. This increase is essentially located in the green-red wavelengths (500 – 670 nm), where it can reach 20%, and is expressed as a shift of the REP toward shorter wavelengths around 700 nm. In comparison, the blue wavelengths (400 – 500 nm) are weakly affected. This response is observed after few days of exposure – even at low concentration – and becomes more pronounced in time, making crude oil and petroleum products more easily detectable. Once again, it is difficult to identify the most contributing hydrocarbons and HMs, since a single of these compounds is able to induce a similar response [146,184,185].

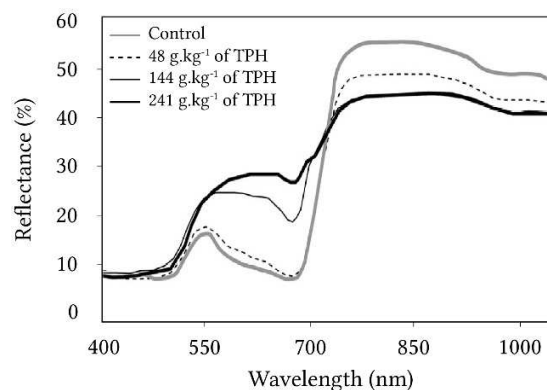


Figure 9. Spectral signatures of leaves of *Zea mays* L. grown for 14 days on engine oil-contaminated (48 – 214 g.kg<sup>-1</sup>) or uncontaminated soils (modified from [59]).

Although the increase of green-red reflectance and the shift of the REP are frequent, an absence of reflectance change has been sometimes observed in studies (Table 2) [16,139,186]. In addition, some oil-tolerant species exhibit modifications of reflectance in the first stages of exposure to oil, and then recover reflectance values similar than those of healthy plants [57].

Other species are even stimulated by low TPH concentrations, inducing a decrease in reflectance [172]. This underlines the variability of vegetation response to crude oil and petroleum products discussed in section 3.4. Of the mentioned studies, some clearly linked the level of pigment content alteration to that of reflectance in the VIS [49,57,183]. They focused on leaf chlorophyll content, because of its major influence on reflectance in the 500 – 670 nm wavelengths [183]. Sanches *et al.* [58,165] conducted an experiment on four oil-sensitive species exposed to gasoline and diesel and concluded that carotenoid content had only few contribution to reflectance changes in the VIS. Conversely, these pigments were highly involved in the response of oil-tolerant species in other studies [57,172].

As described in section 2.2, reflectance in the NIR is highly dependent on the species – especially mono- and dicotyledonous – and on the acquisition scale (leaf, canopy). The same factors, as well as mixture composition, lead to contrasted response of vegetation in this region (Table 2). Whether they result from an increase or a decrease of reflectance, differences between healthy and affected vegetation can exceed 20% in the NIR [58]. A decrease in reflectance is more likely to be observed at canopy scale, since plant development – and thus LAI – is strongly limited by hydrocarbons and HMs. However, several exceptions have been noticed in the literature. As pointed out by three studies [57,58,139], a single species can undergo opposite reflectance changes in the NIR, depending on the crude oil or petroleum product to which it is exposed. Likewise, two species exposed to a similar concentration of the same petroleum product can exhibit contrasted responses in this region [187]. This causes serious detection limits in regions with high species diversity. Similar observations have been made at leaf scale, where reflectance in the NIR mainly depends on anatomy. However, no study demonstrated the relationship between alterations of parenchyma and reflectance changes in this region.

Because of modifications in vegetation water status, the SWIR is largely impacted by exposure to crude oil and petroleum products. As well as in the NIR, the response of vegetation in the SWIR varies among studies (Table 2). In the case where a decrease of reflectance is observed on exposed vegetation, it remains rarely lower than 10% [188]. Conversely, an increase of reflectance, which is more consistent with the reduction of leaf water content and canopy LAI, can exceed 20% for the most oil-sensitive species. In both cases, the response appears later than in the VIS and is thus a good indicator of a long-term exposure. As expected, the most affected wavelengths are located in water absorption features [183]. Because of low atmospheric transmission, these features are however unusable at canopy – and image – scale, but other ones (*e.g.* 1600 and 2200 nm) proved to be good alternatives [57,58]. Vegetation reflectance in the SWIR also depends on celluloses, hemicelluloses, lignins and proteins, which have already been reported as slightly sensitive to petroleum products in one study [58]. Because of the strong influence of LWC in this region, it is unlikely that alterations in these biochemical compounds have major contribution to the modifications of reflectance described here.

Table 2. Effects induced by crude oil and petroleum products on vegetation reflectance in the different spectral regions, at leaf and canopy scales. This review includes studies carried out under experimental or field conditions and implying point reflectance measurements using a spectroradiometer. (VIS: Visible, NIR: Near Infra-Red, SWIR: Short-Wave InfraRed, ↑ and ↓ denotes reflectance increase and decrease, respectively; FC: Field capacity; \* indicates dose-dependent effects; n.a.: not available; n.s.: non-significant effect.)

Species	Conditions	Crude oil petroleum product	TPH	Total time of exposure	Reflectance - Leaf scale			Reflectance - Plant / Canopy scale			Ref.
					VIS	NIR	SWIR	VIS	NIR	SWIR	
<i>Brachiaria brizantha</i>	Field	Diesel	12.7 L.m <sup>-3</sup>	30 days	↑*	↑*	↑*	↑*	↑*	↑*	[58]
	Field	Gasoline	12.7 L.m <sup>-3</sup>	30 days	↑*	↓*	↑*	↑*	↓*	↑*	
<i>Buddleja davidii</i> Franch.	Field	Mud pit	16-77 g.kg <sup>-1</sup>	n.a. <sup>a</sup>	n.s.	n.s.	n.s.	n.a.	n.a.	n.a.	[49]
<i>Cenchrus alopecuroides</i> (L.)	Experimental	Mud pit	14 g.kg <sup>-1</sup>	60 days				↑	↓	↑	[56]
<i>Cenchrus alopecuroides</i> (L.)	Experimental	Mud pit	1-19 g.kg <sup>-1</sup>	42 days	↑*	↑*	↑*	↑*	↑*	↑*	[172]
<i>Cornus sanguinea</i> L.	Field	Mud pit	16-77 g.kg <sup>-1</sup>	n.a. <sup>a</sup>	↑*	↑*	↑*	n.a.	n.a.	n.a.	[49]
<i>Forsythia suspensa</i>	Experimental	Engine oil	20-60 % soil FC	28 days	↑*	↑	n.a.				[187]
<i>Neonotonia wightii</i>	Field	Diesel	6.25 L.m <sup>-3</sup>	184 days	↑*	↓*	↓*	↑*	↓*	↓*	[188]
	Field	Gasoline	6.25 L.m <sup>-3</sup>	184 days	↑*	↓*	↓*	↑*	↓*	↓*	
<i>Panicum virgatum</i> L.	Experimental	Mud pit	14 g.kg <sup>-1</sup>	60 days	n.a.	n.a.	n.a.	↑	↓	↑	[56]
<i>Pennisetum alopecuroides</i>	Experimental	Engine oil	20-60 % soil FC	28 days	↑*	↓*	n.a.	n.a.	n.a.	n.a.	[187]
<i>Phragmites australis</i>	Field	Oil well leak	9.45-652 mg.kg <sup>-1</sup>	n.a. <sup>a</sup>	n.a.	n.a.	n.a.	↑*	↓*	n.a.	[189]
<i>Populus x canadensis</i> Moench.	Field	Mud pit	16-77 g.kg <sup>-1</sup>	n.a. <sup>a</sup>	↑*	↑*	↑*	n.a.	n.a.	n.a.	[49]
<i>Quercus pubescens</i> Wild.	Field	Mud pit	16-77 g.kg <sup>-1</sup>	n.a. <sup>a</sup>	↑*	↑*	↑*	n.a.	n.a.	n.a.	[49]
<i>Rubus fruticosus</i> L.	Experimental	Mud pit	4-40 g.kg <sup>-1</sup>	100 days	↑	↑	↑	↑	↑	↑	[16]
<i>Rubus fruticosus</i> L.	Experimental	Mud pit	36 g.kg <sup>-1</sup>	60 days	↑	↑	↑	↑	↑	↑	[56]
<i>Rubus fruticosus</i> L.	Experimental	Mud pit	6-25 g.kg <sup>-1</sup>	32 days	↑ or n.s.*	↑ or ↓*	↑ or ↓*	↑ or n.s.*	↓*	↑ or ↓*	[57]
	Experimental	Crude oil	25 g.kg <sup>-1</sup>	32 days	↑	↑	↑	↓	↓	↑	
<i>Rubus fruticosus</i> L.	Field	Mud pit	16-77 g.kg <sup>-1</sup>	n.a. <sup>a</sup>	↑*	↑*	↑*	n.a.	n.a.	n.a.	[49]
<i>Salicornia virginica</i>	Experimental	Alba' crude oil	7.7-9.1 %	32 days	n.s.	↑	n.a.	n.a.	n.a.	n.a.	[139]

<sup>a</sup> Naturally-established vegetation



	Experimental	Escravos' crude oil	0.7-1.4 %	32 days	↓	↓	n.a.	n.a.	n.a.	n.a.	
Species	Conditions	Crude oil petroleum product	TPH	Total time of exposure	Reflectance - Leaf scale			Reflectance - Plant / Canopy scale			Ref.
					VIS	NIR	SWIR	VIS	NIR	SWIR	
<i>Triticum sp.</i>	Experimental	Gasoline	10-100 ml.kg <sup>-1</sup>	106 days	n.s.	n.s.	n.s.	n.a.	n.a.	n.a.	[186]
<i>Zea mays</i>	Field	Diesel	6.25 L.m <sup>-3</sup>	184 days	↑*	↓*	↓*	n.a.	n.a.	n.a.	[188]
	Field	Gasoline	6.25 L.m <sup>-3</sup>	184 days	↑*	↓*	↓*	n.a.	n.a.	n.a.	
<i>Zea mays</i>	Experimental	Engine oil	48-241 g.kg <sup>-1</sup>	14 days	↑*	↓*	n.a.	n.a.	n.a.	n.a.	[59]
<i>Zea mays</i>	Experimental	Mud pit	4-40 g.kg <sup>-1</sup>	100 days	n.s.	↓	↑	n.a.	n.a.	n.a.	[16]
<i>Zea mays</i>	Field	Gasoline	8.33 L.m <sup>-3</sup>	203 days	↑*	↓*	↓*	n.a.	n.a.	n.a.	[188]
	Field	Diesel	8.33 L.m <sup>-3</sup>	203 days	↑*	↓*	↓*	n.a.	n.a.	n.a.	
<i>Zea mays</i>	Experimental	Engine oil	96 g.kg <sup>-1</sup>	20 days	↑	↑	↑	n.a.	n.a.	n.a.	[116]

#### 4.2. Methods developed for detecting crude oil and petroleum products under controlled and field conditions

The studies carried out to characterize the spectral response of vegetation to crude oil and petroleum products gave rise to various methods for detecting and quantifying TPH. These methods are based on exploiting the modifications of reflectance described in section 4.1, under controlled or field conditions. Most of existing methods rely on visual or statistical comparisons of spectral signatures between healthy and oil-exposed vegetation [16,139]. These methods are however limited for application beyond the context studied. Other authors exploited reflectance at particular wavelengths by using VI, REP and spectrum transformations, and converged on the critical importance of VIS wavelengths [58,59,183]. Gürtler *et al.*[188] compared these methods for discriminating among healthy and gasoline- or diesel-exposed vegetation, at leaf and canopy scales, and concluded that their performance depends on the species. In a single experiment, Sanches *et al.* [58] combined first derivative and *continuum* removal spectra transformation to Principal Component Analysis (PCA) for similar purpose and identified the red-edge region as a good indicator of soil contamination. However, none of the above-mentioned methods aimed to predict whether vegetation is – or has been – exposed to crude oil or petroleum products from its spectral signature. This represents an important issue for detecting contamination under natural conditions without *a priori* knowledge about their presence.

VI, REP and spectrum transformations have been used for assessing stress-induced alterations in vegetation health in a wide range of contexts. Filella & Peñuelas [81] used reflectance derived in the red-edge for tracking changes in LCC and LAI of *Capsicum annuum* and *Phaseolus vulgaris* resulting from nitrogen deficiencies. Likewise, VI exploiting the NIR and SWIR regions succeeded in tracking water-stress caused by insufficient irrigation or pests [120,190]. When

used in classification or simple and multiple regression methods, these reflectance data allow predicting stressed vegetation and quantifying biophysical and biochemical parameters automatically [191–194]. Therefore, they are great candidates for detecting crude oil and petroleum products and quantifying TPH indirectly.

Classification relies on the combination of several discrete or continuous variables (*e.g.* reflectance data, VI) to predict a categorical response variable (*e.g.* “healthy” or “stressed”) through a mathematical function [195]. Here, we only consider supervised classification. In most cases, these methods are first calibrated on a set of data with known categories, called the *training set*, and tested on an independent set – the *test set* - by predicting categories and comparing them to the true ones [196]. Numerous classification methods have been proposed in the literature [197–199]. When dealing with hyperspectral data, several constraints yet arise. Since reflectance is measured over multiple and contiguous wavelengths, it is not rare to have more variables than observations (*i.e.* reflectance wavelengths > sample size). This phenomenon, known as the Hughes’ effect [200], leads to overfitting of the training set, which negatively affects classification accuracy. This effect can be partly avoided by reducing the dimensionality of the variables using, for example, Principal Component Analysis (PCA). Focusing on vegetation studies, Linear Discriminant Analysis (LDA), Support Vector Machines (SVM), Random Forest (RF) and Spectral-Angle-Mapper-based classification (SAM) revealed to be particularly efficient for discriminating healthy and stressed categories while avoiding overfitting [192,194,201,202]. However, an exhaustive review proposed by Lowe *et al.* [179] stated that no consensus is made in the choice of the method, since their performance highly depends on the purpose of the classification. Few methods allow identifying the most important (*i.e.* discriminant) variables through weighting or stepwise selection criteria [201,203]. Stepwise

Forward LDA [204] has been specifically designed for this purpose, but remains poorly adapted to hyperspectral data because of high multicollinearity. In a spectral region, multicollinearity occurs when reflectance data are linear combination of each other [205]. For example, correlation coefficients ( $r$ ) among reflectance data from different red wavelengths can easily exceed 0.8, which indicates high redundancy. Variable selection becomes very difficult in this case. To achieve it, penalized methods have been developed, such as the Elastic net [206], but remain underexploited in vegetation studies.

Regression methods are used to predict a continuous response variable from one (simple regression) or several (multiple regression) continuous input variables [207]. In practice, these methods follow the same calibration – test procedure than for classification. Simple regression relies on the calibration of univariate models (*e.g.* polynomial, exponential, etc.). It has been especially used for predicting LCC from single VI in previous studies [64,67,81]. Multiple regression regroups a wide range of methods that do not substantially differ from classification ones, and are constrained by the same overfitting and multicollinearity issues. Regarding vegetation studies, it has been shown that Stepwise LDA, Partial Least Square Regression (PLSR) and Support Vector Regression (SVR) are well-suited for retrieving biophysical and biochemical parameters from hyperspectral data [191,193,208]. Once again, there is no best method since the performance varies according to the context. Since both classification and regression methods perform well for detecting and quantifying stress-induced changes in vegetation health, they are promising for monitoring oil contamination from vegetation reflectance. Studies listed in Table 2 showed that the mixture composition and the overall TPH concentration strongly influence the amplitude of reflectance modifications observed in the whole spectral signature. Based on these observations, predictive methods combining VI and

either classification and regression approaches have been recently proposed to detect and characterize oil (*i.e.* to identify the type of crude oil or petroleum product) and to quantify TPH concentration in temperate and tropical regions [57,172]. These methods rely on tracking subtle changes in chlorophyll or various carotenoid contents induced by oil contamination by exploiting reflectance at multiple wavelengths in the VIS. They proved suitable for use both under controlled conditions and in the field.

Other methods based on a different approach have been developed for similar purposes. Those based on RTM are of great interest. RTM are physically-based models aiming to simulate vegetation optical properties. They are typically classified in four categories: plate models, N-flux models, stochastic models and ray tracing models [98,209]. Focusing at leaf scale, the plate model PROSPECT is probably the most widespread [52,72]. In its direct mode, PROSPECT allows simulating leaf optical properties (reflectance and transmittance) in the optical reflective domain from its biophysical and biochemical parameters (structure and pigment, water and dry matter contents). Inversion of the model allows retrieving these parameters from reflectance and transmittance measurements performed on leaves [125]. PROSPECT has been used in many studies dealing with environmental monitoring purposes [72,210]. While LCC and LWC remain the most targeted parameters in vegetation stress assessment [119,211], recent improvements of the model allow separating chlorophylls, carotenoids and anthocyanins with good precision [68,92]. In a recent study, Arellano *et al.* [48] inverted the model to compare LCC of various tropical plant families among uncontaminated and oil-spill sites, and found significant alterations for some of them. More recently, Lassalle *et al.* [49] inverted PROSPECT to retrieve oil-induced chlorophyll alterations in leaves from reflectance data, making possible to quantify TPH concentrations in soils (Figure 10). These two studies also highlighted the importance of taking

the species' sensitivity to oil and the development stage into account, which both determine the detection and quantification accuracy.

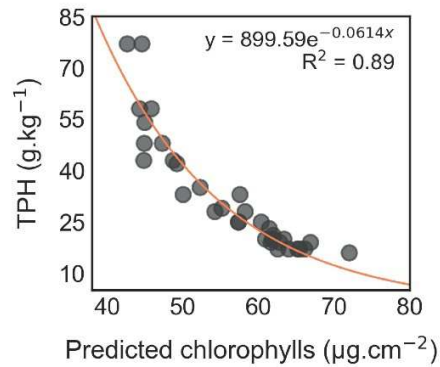


Figure 10. Relationship between Leaf Chlorophyll Content (LCC) retrieved from the spectral signature of *Rubus fruticosus* L. by inverting the PROSPECT model, and the concentration of Total Petroleum Hydrocarbons (TPH) in mud pit soils [49].

Hence, the methods developed for monitoring oil contamination from vegetation reflectance are largely inspired from those of other fields (agronomy, ecology). In a perspective of application at large scale – using airborne or satellite imagery, an upscaling of these methods is necessary. This represents a difficult step to cross toward operational applications over industrial facilities.

## 5. Application in contamination monitoring using airborne and satellite imagery

### 5.1. Synthesis based on previous studies

Few attempts have been made in detecting oil leakages and contaminated mud pits in vegetated areas using optical remote sensing in the past (Table 3). In most cases, studies aimed to assess the impact of crude oil and petroleum products on the environment using multi- (Landsat) or

hyperspectral (Hyperion) satellite imagery at 30-m spatial resolution [23,212–214]. More rarely, the goal was to detect natural oil seepages (Figure 11a-b) [55]. A limited number of authors have used airborne hyperspectral images, and those who did have rarely exploited the entire spectral signature of vegetation. Almost all the mentioned studies used REP or VI to detect changes in vegetation health induced by crude oil or petroleum products. As for experiments carried out under controlled conditions, these methods rely on mean comparison between sites with healthy and oil-exposed vegetation [54,212,215]. They proved to be efficient for identifying vegetation stress on seepage or leakage sites, but suffered from serious limits when applied outside the study area (Figure 11a-b).

Table 3. Studies aiming to detect and quantify crude oil and petroleum products using multi- and hyperspectral airborne and satellite images. (Refl.: Reflectance; VI: Vegetation Indices; CR: *Continuum* Removal; RF: Random Forest; REP: Red-Edge Position; comp.: Comparison; RTM: Radiative Transfer Model.)

Vegetation type	Target	Sensor name	Sensor type (spatial resolution)	Bands (spectral domain)	Method	Ref.
<b>Multispectral</b>						
Mangrove	Crude oil leakage	Landsat-8	Satellite (30 m)	9 (435 - 2294 nm)	VI + Mean comp.	[212]
Crops, grassland & trees	Crude oil leakage	Landsat-8	Satellite (30 m)	9 (435 - 2294 nm)	VI + RF classification	[213]
Mangrove	Crude oil leakage	Landsat-5 & -7	Satellite (30 m)	6 (450 - 2350 nm)	VI + Simple regression	[216]
Mangrove	Crude oil leakage	Landsat-5 & -7	Satellite (30 m)	6 (450 - 2350 nm)	VI + Mean comp.	[216]
<b>Hyperspectral</b>						
Wetland	Crude oil leakage	AISA	Airborne (1.5 m)	286 (400 - 2400 nm)	Reflectance + Classification	[217]
Crops	Benzene pipeline leak	HyMap	Airborne (4 m)	128 (436 - 2485 nm)	REP & VI + Spatial filter	[23]
Temperate shrubs	Mud pit	HySpex	Airborne (1 m)	409 (400 – 2500)	VI + Classification RTM + Regression	[50]
Mediterranean grassland	Crude oil microseepage	Probe-1	Airborne (8 m)	128 (436 - 2480 nm)	REP & VI + Spatial filter	[55]
Tropical forest	Crude oil leakage	Hyperion	Satellite (30 m)	242 (400 - 2500 nm)	VI + Threshold	[54]
Plain & rainforest	Crude oil leakage	Hyperion	Satellite (30 m)	242 (400 - 2500 nm)	CR + Mean comp.	[215]
Plain & rainforest	Crude oil leakage	Hyperion	Satellite (30 m)	242 (400 - 2500 nm)	Refl. & VI + Mean comp.	[215]

In contrast to experimental studies, REP and VI have already been exploited in classification or anomaly detection methods on multi- and hyperspectral images. However, the performance of

these methods has been rarely quantified. Their evaluation mostly relied on visual interpretation of detection mapping with lacking ground validation data, which are often difficult to obtain. Among notable examples, Ozigis *et al.* [213] combined 10 VI in random forest on 30-m resolution Landsat-8 images for detecting oil leakages and obtained an overall accuracy of maximum 70% on selected sites. Conversely, Arellano *et al.* [54] applied successive vegetation index thresholds to map oil-induced stress near production facilities using 30-m resolution Hyperion images. These methods were first calibrated on a study area, and then applied to the entire image. In all cases, they led to the apparition of false alarms, especially false positives (*i.e.* vegetation stress not induced by petroleum hydrocarbons and HMs) (Figure 11b). This phenomenon is observed under various contexts (*e.g.* temperate, tropical) and results from multiple factors. First, in most studies, the spatial resolution of the images was not adapted to the size of the target. In addition, as described in section 3.4, certain species are particularly tolerant to crude oil and petroleum products and undergo only little changes in their spectral signature, which make them difficult to discriminate from healthy vegetation. In that situation, high spectral resolution and signal-to-noise ratio are needed to catch these changes in reflectance, so hyperspectral sensors are required. In addition, natural differences in optical properties among species and individuals – as well as in sensitivity to oil – make the detection particularly challenging in areas with high species diversity. For instance, a species exposed to crude oil or petroleum products may exhibit a similar spectral signature than that of another unexposed species [49]. This becomes a serious issue at decametric spatial resolution, where species are highly mixed inside pixels. A similar issue arises when exposed species are mixed with bare soil. Very high spatial resolution (1 – 2 m) is thus needed to overcome these limits.



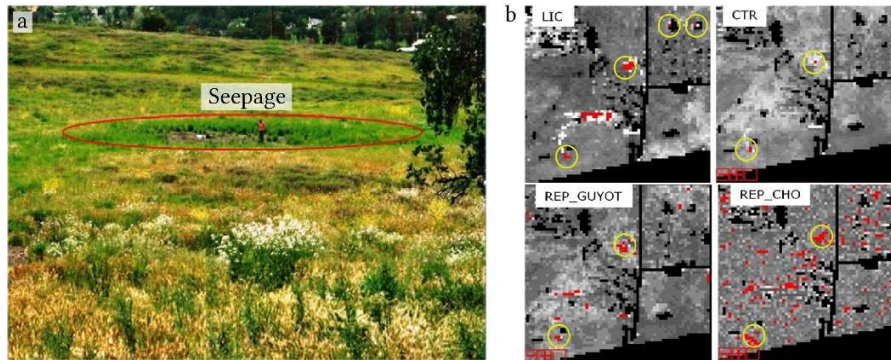


Figure 11. (a) Crude oil seepage in vegetated area. The seepage is surrounded by a particular vegetation distribution pattern, which allows being detected (b) from hyperspectral airborne images using various vegetation indices (see [55] for the description of indices). However, false alarms (red pixels outside yellow circles) cannot be avoided. Similar observations have been depicted for accidental oil leakages [54,216].

Ozigis *et al.* [213] pointed out several sources of confusion that contribute to increasing false positives. The presence of crude oil and petroleum products is not the only factor affecting vegetation health and optical properties under natural conditions. Some biotic or abiotic factors are likely to induce similar effects, thus introducing confusion. As described in section 3.2, crude oil and petroleum products reduce water availability for plants and can induce a water-deficit stress. Under natural conditions, this effect can be easily confused with that of a “natural” water-deficit (*i.e.* resulting from insufficient precipitation and/or highly drained soils). Although it seems possible to discriminate these stressors for highly oil-sensitive species under controlled conditions [59,183], it is more difficult for oil-tolerant species and using airborne or satellite hyperspectral images. Stress confusion has been identified as one of the most important cause of misclassification in previous studies. It is therefore necessary to account for these sources of confusion in each context, when applying detection methods over an entire region. Once again,

very high spatial and spectral resolutions are needed to achieve efficient discrimination of oil and other stressors. Although no current satellite-embedded sensor offers such resolutions simultaneously at the moment, airborne imagery represents a good alternative [217].

As concluded from the above-mentioned studies, it is not the best option to develop methods for detecting and quantifying oil using only airborne or satellite images, especially without solid knowledge about the context (species' sensitivity, hydrocarbon and HM mixture, other potential stressors). Experiments carried out under controlled conditions are a necessary first step, since they help determining the response of vegetation specifically induced by crude oil and petroleum products. These experiments must be representative of realistic field conditions (*i.e.* species, TPH concentrations) and serve as basis for developing classification or regression methods that are suitable for use on images. The upscaling of methods is the most important difficulty in this approach, so it is crucial to address it progressively; for example, from leaf to canopy scales and finally on images. The validation of the methods in the field is an intermediate – and critical – step prior to imagery application. Then, the methods should be progressively applied to imagery; first, on selected sites with known species' sensitivities, and thereafter at large scale. This multiscale approach proved efficient in recent studies. For example, Lassalle *et al.* [49,50,57] developed methods for detecting and quantifying TPH based on bramble reflectance under controlled and field conditions and succeeded in applying them on airborne hyperspectral images over contaminated mud pits (accuracy > 90%).

The studies listed in Table 3 demonstrated the feasibility of assessing oil contamination using optical remote sensing. However, the methods described in these studies were validated locally, in a specific context. As a perspective, they are intended to be applied operationally in a broader range of situations encountered in oil contamination monitoring (pipeline leakage, mud pits,

storage tanks failure, etc.), in various regions (temperate, tropical, etc.). This implies extending the scope of these methods and overcoming their current limits regarding operating and future satellite-embedded sensors.

## 5.2. Perspectives toward operational applications in oil and gas industry

In an operational context, remote sensing should provide accurate mapping of oil over large industrial facility sites colonized by vegetation. At this stages, the methods developed for this purpose remain rarely effective – or often unassessed – outside a given study site [54,55,213], which limits their operational use. Most of them are adapted to a given species or vegetation type (mangroves, shrubs, etc.) with known location, so these methods can be applied for identifying new contaminated sites, provided they are colonized by the same species or vegetation type. This remains very restrictive, because oil can be mapped only locally and to pre-selected vegetated sites. Therefore, in an operational perspective, it is essential to extend the scope of the methods to other contexts (in terms of species and contamination type and level). Likewise, they should be applicable to entire images, in order to assess oil contamination at large scale. To achieve this, it is not conceivable to use airborne hyperspectral imagery – especially for daily monitoring, because it implies an important economic cost. Conversely, satellite imagery is already used operationally by oil and gas companies for mineralogical mapping and marine oil spill tracking [218,219]. Satellite-embedded sensors can provide images over industrial facilities on a daily – or weekly – basis, allowing continuous monitoring of oil contamination. To date, the best spatial resolution provided by operating and planned hyperspectral satellite-embedded sensors is 8 m, with less than 300 spectral bands in the reflective domain (Table 4). In contrast, the best methods developed for assessing oil contamination were developed using high to very high spatial and

spectral resolutions [23,50,217]. Using satellite imagery, their performance would be impacted by the degradation of resolutions. Therefore, two conditions are required for applying these methods in an operational way, namely: extending their scope to a wide range of contexts and adapting them to future satellite-embedded hyperspectral sensors (Table 4).

Table 4. Specifications of operational and future satellite-embedded hyperspectral sensors. The name and specifications of future sensors may be modified until their operating (n.a.: not available).

Sensor name	Spectral domain (nm)	Bands	Spatial resolution (m)	Launch date
CHRIS	415 - 1050	19-63	18-36	operational
EnMAP	420 - 2450	244	30	2020
HISUI	400 - 2500	185	30	2020
HJ-1A	450 - 950	115	100	operational
Hyperion	357 - 2576	220	30	operational
HypXim	400 - 2500	210	8	2020-2022
HySI	400 - 950	64	550	operational
HypIRI VSWIR	380 - 2500	212	30	n.a.
PRISMA	400 - 2505	249	30	operational
SHALOM	400 - 2500	275	10	2020
TianGong-1	400 - 2500	128	10-20	operational

At this stage, the application of the methods at large scale is limited by the necessity to know the location of the species – or vegetation type – on images. In an operational frame, an automatic mapping of this species would be helpful. Without this preliminary step, the methods would lead to false-detection alarms and inaccurate quantification of TPH if applied to other species and vegetation types, which differ in optical properties and sensitivity to oil [50,55,220]. The mapping could be achieved quite easily for homogenous and dense covers, but would become harder in regions with high species richness. It is particularly true when using satellite imagery, as “pure” pixels of dense vegetation (*i.e.* including a single species or vegetation type and no bare soil) become even rarer with increasing spatial resolution. Spectral unmixing might help overcoming this issue [47]. Unmixing aims at identifying the different species or vegetation

types inside pixels using, for example, spectral libraries. Lots of unmixing methods have been proposed in previous studies [47,221–223]. Focusing on vegetation studies, unmixing methods have been developed for two main purposes: mapping a single target species or vegetation type and discriminating among various ones. Thus, unmixing could be used for mapping the species or vegetation types of interest before applying the methods of oil detection and quantification. Toward operational monitoring, future studies should focus on applying unmixing methods prior to detecting and quantifying TPH at satellite spatial resolution. However, it might be interesting not to limit to the species or vegetation types on which the methods were developed. Various species might serve for detecting and quantifying oil, which would extend the scope of the methods and fulfill operational needs.

Once the target species or vegetation types have been mapped, it is important to note that the accuracy of the detection and quantification of oil will depend on the level of contamination. For example, the exact range of effectiveness of the methods proposed for quantifying TPH remains unknown [49,50,189]. This information is essential for operational applications, because oil contamination can extend to a wide range of concentrations. Further studies should focus on determining the exact limits of detection and quantification of existing methods, especially since they may vary among species. Depending on their sensitivity to oil, all species do not allow detecting and quantifying contamination in the same range. Species with different sensitivities could be complementary for quantifying TPH over a wide range of concentrations [49,189,220]. High spatial resolution is also needed, as TPH concentrations may vary locally. 8- or 30-m pixels may include different species exposed to different levels of contamination, making oil very difficult to detect and quantify accurately. Hence, an important effort remains to identify the

species suitable for monitoring oil contamination and to define their respective range of effectiveness at the spatial resolution of satellite-embedded sensors.

At this stage, the scope of the methods developed for detecting and quantifying TPH is restricted to assessing huge oil leakages (e.g. major oil spills and large, contaminated mud pits). Toward operational applications, it should extend to other scenarios. Chronic crude oil or petroleum product leaks deriving from pipeline or storage tank failures are priority, because they represent one of the main sources of contaminant release from oil industry [15,18]. From the perspective of satellite imagery application, one possible limit to applying the methods may arise at the spatial resolution of satellite images for small contaminated areas. More precisely, pipeline and storage tank leaks can spread on a few square meters [35,43], making their detection challenging at satellite spatial resolution, because pixels would not only include oil-exposed vegetation. Therefore, the required spatial resolution depends on the contamination event to detect (mud pit, pipeline leak, etc.).

## 6. Conclusion

This review aimed at summarizing the advances and challenges in using optical remote sensing for assessing oil contamination in vegetated areas. Although the optical properties of vegetation have been well documented, their use in oil and gas industry is still recent. By exploiting modifications in these properties caused by pigment and water alteration in leaves, previous studies have shown that it is possible to detect and quantify TPH in soils under controlled and field conditions. However, at this stage, several limits discussed in this review prevent from applying the same methods in an operational way at large scale, using hyperspectral imagery. Hence, the work summarized in this review should continue in further research, in order to

extend the scope of the methods and to assess their operational maturity. More precisely, future studies should first focus on identifying more relevant plant species and, for each of them, the types of oil (*i.e.* crude oil and petroleum products) and the range of concentrations that can be detected or quantified. This would be helpful for remote sensing operators of oil and gas companies, as the methods could be used for a wide range of purposes in oil exploration and contamination monitoring. Prior to operational applications, the methods should be evaluated at the spatial and spectral resolutions of future satellite-embedded hyperspectral sensors, along with species unmixing.

On the long term, oil and gas companies may spark growing interest in UAV-embedded hyperspectral sensors. Although they are still under development, they represent a promising complement or alternative to satellite imagery. UAV-embedded sensors allow multitemporal, localized, monitoring, while providing very high spatial (up to cm scale) and spectral resolutions [224,225], therefore overcoming some of the above-mentioned limits. In addition, active remote sensing could be used to improve oil detection and quantification, by providing complementary information about vegetation. For example, radar and LiDAR imagery are useful for estimating canopy height and biomass [226], which are affected by oil. Radar remote sensing is light-independent and atmospherically-resistant, which is a considerable advantage in wet tropical regions [227,228]. By combining various technologies (active and passive) and sensor platforms (satellite, drone), remote sensing will undoubtedly become an indispensable support to oil contamination monitoring in vegetated areas in the coming decades.

## Acknowledgements

This work was performed in the frame of the NAOMI project between TOTAL and the ONERA, with the support of the Ecolab research unit in Toulouse.

Declarations of interest: None.

Funding: Financial support of this work was provided by TOTAL.

## References

- [1] G.A. Marrero, Greenhouse gases emissions, growth and the energy mix in Europe, *Energy Econ.* 32 (2010) 1356–1363. doi:10.1016/j.eneco.2010.09.007.
- [2] L. Suganthi, A.A. Samuel, Energy models for demand forecasting - A review, *Renew. Sustain. Energy Rev.* 16 (2012) 1223–1240. doi:10.1016/j.rser.2011.08.014.
- [3] G.A. Jones, K.J. Warner, The 21st century population-energy-climate nexus, *Energy Policy.* 93 (2016) 206–212. doi:10.1016/j.enpol.2016.02.044.
- [4] R.G. Miller, S.R. Sorrell, H. Lane, S. Kt, The future of oil supply, *Philos. Trans. R. Soc. A.* 372 (2014) 20130179. doi:10.1098/rsta.2013.0179.
- [5] OPEC, The Organization of the Petroleum Exporting Countries Annual Report 2017, (2018).  
[https://www.opec.org/opec\\_web/static\\_files\\_project/media/downloads/publications/AR2017.pdf](https://www.opec.org/opec_web/static_files_project/media/downloads/publications/AR2017.pdf).
- [6] C. Zou, Q. Zhao, G. Zhang, B. Xiong, Energy revolution: From a fossil energy era to a new energy era, *Nat. Gas Ind. B.* 3 (2016) 1–11. doi:10.1016/j.ngib.2016.02.001.
- [7] R.W. Bentley, Oil Forecasts, Past and Present, *Energy Explor. Exploit.* 20 (2002) 481–



853 491. doi:10.1260/014459802321615108.

854 [8] P.M. Jackson, L.K. Smith, Exploring the undulating plateau: the future of global oil  
855 supply, *Philos. Trans. R. Soc. A Math. Phys. Eng. Sci.* 372 (2013).  
856 doi:10.1098/rsta.2012.0491.

857 [9] S. Sorrell, J. Speirs, R. Bentley, A. Brandt, R. Miller, Global oil depletion: A review of the  
858 evidence, *Energy Policy*. 38 (2010) 5290–5295. doi:10.1016/j.enpol.2010.04.046.

859 [10] S. Sorrell, R. Miller, R. Bentley, J. Speirs, Oil futures: A comparison of global supply  
860 forecasts, *Energy Policy*. 38 (2010) 4990–5003. doi:10.1016/j.enpol.2010.04.020.

861 [11] A.E. Ite, U.J. Ibok, M.U. Ite, S.W. Petters, Petroleum Exploration and Production: Past  
862 and Present Environmental Issues in the Nigeria's Niger Delta, *Am. J. Environ. Prot.* 1  
863 (2013) 78–90. doi:10.12691/env-1-4-2.

864 [12] U.S. Energy Information Administration (EIA), Definitions of Petroleum Products and  
865 Other Terms, 2010.

866 [13] H.H. Lean, R. Smyth, Long memory in US disaggregated petroleum consumption:  
867 Evidence from univariate and multivariate LM tests for fractional integration, *Energy*  
868 *Policy*. 37 (2009) 3205–3211. doi:10.1016/j.enpol.2009.04.017.

869 [14] J. Solé, A. García-Olivares, A. Turiel, J. Ballabrera-Poy, Renewable transitions and the  
870 net energy from oil liquids: A scenarios study, *Renew. Energy*. 116 (2018) 258–271.  
871 doi:10.1016/j.renene.2017.09.035.

872 [15] J.I. Chang, C.C. Lin, A study of storage tank accidents, *J. Loss Prev. Process Ind.* 19  
873 (2006) 51–59. doi:10.1016/j.jlp.2005.05.015.

874 [16] A. Credo, R. Hédacq, C. Barreau, D. Dubucq, Experimental study of hyperspectral  
875 responses of plants grown on mud pit soil, in: *Earth Resour. Environ. Remote*

876 Sensing/GIS Appl. VII, 2016: p. 100051E. doi:10.1117/12.2239606.

877 [17] B.K. Gogoi, N.N. Dutta, P. Goswami, T.R. Krishna Mohan, A case study of  
878 bioremediation of petroleum-hydrocarbon contaminated soil at a crude oil spill site, Adv.  
879 Environ. Res. 7 (2003) 767–782. doi:10.1016/S1093-0191(02)00029-1.

880 [18] S.B. da Cunha, A review of quantitative risk assessment of onshore pipelines, J. Loss  
881 Prev. Process Ind. 44 (2016) 282–298. doi:10.1016/j.jlp.2016.09.016.

882 [19] S.R. Shadizadeh, M. Zoveidavianpoor, A drilling reserve mud pit assessment in Iran:  
883 Environmental impacts and awareness, Pet. Sci. Technol. 28 (2010) 1513–1526.  
884 doi:10.1080/10916460903117545.

885 [20] J. Durango-Cordero, M. Saqalli, C. Laplanche, M. Locquet, A. Elger, Spatial Analysis of  
886 Accidental Oil Spills Using Heterogeneous Data: A Case Study from the North-Eastern  
887 Ecuadorian Amazon, Sustainability. 10 (2018) 4719. doi:10.3390/su10124719.

888 [21] F.-R. Ahmadun, A. Pendashteh, L.C. Abdullah, D.R. Awang Biak, S.S. Madaeni, Z.Z.  
889 Abidin, Review of technologies for oil and gas produced water treatment, J. Hazard.  
890 Mater. 170 (2009) 530–551. doi:10.1016/j.jhazmat.2009.05.044.

891 [22] G. Hu, J. Li, G. Zeng, Recent development in the treatment of oily sludge from petroleum  
892 industry: A review, J. Hazard. Mater. 261 (2013) 470–490.  
893 doi:10.1016/j.jhazmat.2013.07.069.

894 [23] H. van der Werff, M. van der Meijde, F. Jansma, F. van der Meer, G.J. Groothuis, A  
895 Spatial-Spectral Approach for Visualization of Vegetation Stress Resulting from Pipeline  
896 Leakage, Sensors. 8 (2008) 3733–3743. doi:10.3390/s8063733.

897 [24] F. Barraza, L. Maurice, G. Uzu, S. Becerra, F. López, V. Ochoa-Herrera, J. Ruales, E.  
898 Schreck, Distribution, contents and health risk assessment of metal(loid)s in small-scale

899 farms in the Ecuadorian Amazon: An insight into impacts of oil activities, *Sci. Total*  
900 *Environ.* 622–623 (2018) 106–120. doi:10.1016/j.scitotenv.2017.11.246.

901 [25] X. Bi, B. Wang, Q. Lu, Fragmentation effects of oil wells and roads on the Yellow River  
902 Delta, North China, *Ocean Coast. Manag.* 54 (2011) 256–264.  
903 doi:10.1016/j.ocecoaman.2010.12.005.

904 [26] N.C. Duke, Oil spill impacts on mangroves: Recommendations for operational planning  
905 and action based on a global review, *Mar. Pollut. Bull.* 109 (2016) 700–715.  
906 doi:10.1016/j.marpolbul.2016.06.082.

907 [27] M. Finer, C.N. Jenkins, S.L. Pimm, B. Keane, C. Ross, Oil and gas projects in the Western  
908 Amazon: Threats to wilderness, biodiversity, and indigenous peoples, *PLoS One.* 3  
909 (2008). doi:10.1371/journal.pone.0002932.

910 [28] I.B. Ivshina, M.S. Kuyukina, A. V. Krivoruchko, A.A. Elkin, S.O. Makarov, C.J.  
911 Cunningham, T.A. Peshkur, R.M. Atlas, J.C. Philp, Oil spill problems and sustainable  
912 response strategies through new technologies, *Environ. Sci. Process. Impacts.* 17 (2015)  
913 1201–1219. doi:10.1039/c5em00070j.

914 [29] S. Sorrell, J. Speirs, R. Bentley, R. Miller, E. Thompson, Shaping the global oil peak: A  
915 review of the evidence on field sizes, reserve growth, decline rates and depletion rates,  
916 *Energy.* 37 (2012) 709–724. doi:10.1016/j.energy.2011.10.010.

917 [30] S. Datta, S. Sarkar, A review on different pipeline fault detection methods, *J. Loss Prev.*  
918 *Process Ind.* 41 (2016) 97–106. doi:10.1016/j.jlp.2016.03.010.

919 [31] H.A. Kishawy, H.A. Gabbar, Review of pipeline integrity management practices, *Int. J.*  
920 *Press. Vessel. Pip.* 87 (2010) 373–380. doi:10.1016/j.ijpvp.2010.04.003.

921 [32] A. Shukla, H. Karki, Application of robotics in onshore oil and gas industry—A review

922 Part I, *Rob. Auton. Syst.* 75 (2016) 490–507. doi:10.1016/j.robot.2015.09.012.

923 [33] A. Shukla, H. Karki, Application of robotics in offshore oil and gas industry— A review  
 924 Part II, *Rob. Auton. Syst.* 75 (2016) 508–524. doi:10.1016/j.robot.2015.09.013.

925 [34] A. Al-Sayegh, Enhanced Oil Recovery Using Biotransformation Technique on Heavy  
 926 Crude Oil, *Int. J. GEOMATE*. 13 (2017). doi:10.21660/2017.36.2842.

927 [35] R.E. Correa Pabón, C.R. de Souza Filho, W.J. de Oliveira, Reflectance and imaging  
 928 spectroscopy applied to detection of petroleum hydrocarbon pollution in bare soils, *Sci.*  
 929 *Total Environ.* 649 (2019) 1224–1236. doi:10.1016/j.scitotenv.2018.08.231.

930 [36] O.T. Gudmestad, Sustainable oil and gas production in the 21st century with emphasis on  
 931 offshore fields, *WIT Trans. Ecol. Environ.* 190 (2014) 777–788. doi:10.2495/EQ140722.

932 [37] D. van der Lelie, J.-P. Schwitzguébel, D.J. Glass, J. Vangronsveld, A. Baker,  
 933 Phytoremediation: European and American trends successes, obstacles and needs, *J. Soils*  
 934 *Sediments*. 2 (2008) 91–99. doi:10.1007/bf02987877.

935 [38] A. Necci, S. Girgin, E. Krausmann, Understanding Natech Risk Due to Storms; Analysis,  
 936 Lessons Learned and Recommendations, 2018. doi:10.2760/21366.

937 [39] K. Rehman, A. Imran, I. Amin, M. Afzal, Inoculation with bacteria in floating treatment  
 938 wetlands positively modulates the phytoremediation of oil field wastewater, *J. Hazard.*  
 939 *Mater.* 349 (2018) 242–251. doi:10.1016/j.jhazmat.2018.02.013.

940 [40] Y.-Q. Jin, F. Xu, Polarimetric Scattering and SAR Information Retrieval, John Wiley &  
 941 Sons (Asia) Pte Ltd, Singapore, 2013. doi:10.1002/9781118188149.

942 [41] S. Prasad, L.M. Bruce, J. Chanussot, Optical Remote Sensing; Advances in Signal  
 943 Processing and Exploitation Techniques, Springer Singapore, Singapore, 2019.  
 944 doi:10.1007/978-981-13-2553-3.

- 945 [42] F. Kühn, K. Oppermann, B. Hörig, Hydrocarbon index - An algorithm for hyperspectral  
946 detection of hydrocarbons, *Int. J. Remote Sens.* 25 (2004) 2467–2473.  
947 doi:10.1080/01431160310001642287.
- 948 [43] S. Asadzadeh, C.R. de Souza Filho, Spectral remote sensing for onshore seepage  
949 characterization: A critical overview, *Earth-Science Rev.* 168 (2017) 48–72.  
950 doi:10.1016/j.earscirev.2017.03.004.
- 951 [44] F.D. van der Meer, H.M.A. van der Werff, F.J.A. van Ruitenbeek, C.A. Hecker, W.H.  
952 Bakker, M.F. Noomen, M. van der Meijde, E.J.M. Carranza, J.B. de Smeth, T. Woldai,  
953 Multi- and hyperspectral geologic remote sensing: A review, *Int. J. Appl. Earth Obs.*  
954 *Geoinf.* 14 (2012) 112–128. doi:10.1016/j.jag.2011.08.002.
- 955 [45] E.J. Milton, M.E. Schaepman, K. Anderson, M. Kneubühler, N. Fox, Progress in field  
956 spectroscopy, *Remote Sens. Environ.* 113 (2009) S92–S109.  
957 doi:10.1016/j.rse.2007.08.001.
- 958 [46] T. Slonecker, G.B. Fisher, D.P. Aiello, B. Haack, Visible and infrared remote imaging of  
959 hazardous waste: A review, *Remote Sens.* 2 (2010) 2474–2508. doi:10.3390/rs2112474.
- 960 [47] J.M. Bioucas-Dias, A. Plaza, N. Dobigeon, M. Parente, Q. Du, P. Gader, J. Chanussot,  
961 Hyperspectral unmixing overview: Geometrical, statistical, and sparse regression-based  
962 approaches, *IEEE J. Sel. Top. Appl. Earth Obs. Remote Sens.* 5 (2012) 354–379.  
963 doi:10.1109/JSTARS.2012.2194696.
- 964 [48] P. Arellano, K. Tansey, H. Balzter, D.S. Boyd, Field spectroscopy and radiative transfer  
965 modelling to assess impacts of petroleum pollution on biophysical and biochemical  
966 parameters of the Amazon rainforest, *Environ. Earth Sci.* 76 (2017) 1–14.  
967 doi:10.1007/s12665-017-6536-6.

- 968 [49] G. Lassalle, S. Fabre, A. Credo, R. Hédacq, G. Bertoni, D. Dubucq, A. Elger,  
969 Application of PROSPECT for estimating total petroleum hydrocarbons in contaminated  
970 soils from leaf optical properties, *J. Hazard. Mater.* 377 (2019) 409–417.  
971 doi:10.1016/j.jhazmat.2019.05.093.
- 972 [50] G. Lassalle, A. Elger, A. Credo, G. Bertoni, D. Dubucq, S. Fabre, Toward Quantifying  
973 Oil Contamination in Vegetated Areas Using Very High Spatial and Spectral Resolution  
974 Imagery, *Remote Sens.* 11 (2019) 2241. doi:10.3390/rs11192241.
- 975 [51] G.P. Asner, Biophysical and Biochemical Sources of Variability in Canopy Reflectance,  
976 *Remote Sens. Environ.* 64 (1997) 234–253.  
977 <http://www.sciencedirect.com/science/article/pii/S0034425798000145> 5CnWOS:000074  
978 765100010.
- 979 [52] S. Jacquemoud, F. Baret, PROSPECT: A model of leaf optical properties spectra, *Remote*  
980 *Sens. Environ.* 34 (1990) 75–91. doi:10.1016/0034-4257(90)90100-Z.
- 981 [53] M.R. Slaton, E.R. Hunt, W.K. Smith, Estimating near-infrared leaf reflectance from leaf  
982 structural characteristics, *Am. J. Bot.* 88 (2001) 278–284. doi:10.2307/2657019.
- 983 [54] P. Arellano, K. Tansey, H. Balzter, D.S. Boyd, Detecting the effects of hydrocarbon  
984 pollution in the Amazon forest using hyperspectral satellite images, *Environ. Pollut.* 205  
985 (2015) 225–239. doi:10.1016/j.envpol.2015.05.041.
- 986 [55] M.F. Noomen, H.M.A. van der Werff, F.D. van der Meer, Spectral and spatial indicators  
987 of botanical changes caused by long-term hydrocarbon seepage, *Ecol. Inform.* 8 (2012)  
988 55–64. doi:10.1016/j.ecoinf.2012.01.001.
- 989 [56] G. Lassalle, A. Credo, R. Hédacq, S. Fabre, D. Dubucq, A. Elger, Assessing Soil  
990 Contamination Due to Oil and Gas Production Using Vegetation Hyperspectral

991 Reflectance, *Environ. Sci. Technol.* 52 (2018) 1756–1764. doi:10.1021/acs.est.7b04618.

992 [57] G. Lassalle, S. Fabre, A. Credo, R. Hédacq, P. Borderies, G. Bertoni, T. Erudel, E.

993 Buffan-Dubau, D. Dubucq, A. Elger, Detection and discrimination of various oil-

994 contaminated soils using vegetation reflectance, *Sci. Total Environ.* 655 (2019) 1113–

995 1124. doi:10.1016/j.scitotenv.2018.11.314.

996 [58] I.D. Sanches, C.R. de Souza Filho, L.A. Magalhães, G.C.M. Quitério, M.N. Alves, W.J.

997 Oliveira, Assessing the impact of hydrocarbon leakages on vegetation using reflectance

998 spectroscopy, *ISPRS J. Photogramm. Remote Sens.* 78 (2013) 85–101.

999 doi:10.1016/j.isprsjprs.2013.01.007.

1000 [59] E.J. Emengini, G.A. Blackburn, J.C. Theobald, Early detection of oil-induced stress in

1001 crops using spectral and thermal responses, *J. Appl. Remote Sens.* 7 (2013).

1002 doi:10.1117/1.jrs.7.073596.

1003 [60] F. Wang, J. Gao, Y. Zha, Hyperspectral sensing of heavy metals in soil and vegetation:

1004 Feasibility and challenges, *ISPRS J. Photogramm. Remote Sens.* 136 (2018) 73–84.

1005 doi:10.1016/j.isprsjprs.2017.12.003.

1006 [61] T. Shi, Y. Chen, Y. Liu, G. Wu, Visible and near-infrared reflectance spectroscopy — An

1007 alternative for monitoring soil contamination by heavy metals, *J. Hazard. Mater.* 265

1008 (2014) 166–176. doi:10.1016/j.jhazmat.2013.11.059.

1009 [62] A. Gholizadeh, V. Kopačková, Detecting vegetation stress as a soil contamination proxy:

1010 a review of optical proximal and remote sensing techniques, *Int. J. Environ. Sci. Technol.*

1011 16 (2019) 2511–2524. doi:10.1007/s13762-019-02310-w.

1012 [63] A. Gholizadeh, M. Saberioon, E. Ben-Dor, L. Borůvka, Monitoring of selected soil

1013 contaminants using proximal and remote sensing techniques: Background, state-of-the-art

1014 and future perspectives, *Crit. Rev. Environ. Sci. Technol.* 48 (2018) 243–278.  
 1015 doi:10.1080/10643389.2018.1447717.

1016 [64] D.A. Sims, J.A. Gamon, Relationships between leaf pigment content and spectral  
 1017 reflectance across a wide range of species, leaf structures and developmental stages,  
 1018 *Remote Sens. Environ.* 81 (2002) 337–354. doi:10.1016/S0034-4257(02)00010-X.

1019 [65] A. Vershinin, Biological functions of carotenoids - diversity and evolution, *BioFactors*. 10  
 1020 (1999) 99–104. doi:10.1002/biof.5520100203.

1021 [66] Y. Tanabe, T. Shitara, Y. Kashino, Y. Hara, S. Kudoh, Utilizing the Effective Xanthophyll  
 1022 Cycle for Blooming of *Ochromonas smithii* and *O. itoi* (Chrysophyceae) on the snow  
 1023 surface, *PLoS One*. 6 (2011). doi:10.1371/journal.pone.0014690.

1024 [67] G.A. Blackburn, Spectral indices for estimating photosynthetic pigment concentrations: A  
 1025 test using senescent tree leaves, *Int. J. Remote Sens.* 19 (1998) 657–675.  
 1026 doi:10.1080/014311698215919.

1027 [68] J.B. Feret, C. François, G.P. Asner, A.A. Gitelson, R.E. Martin, L.P.R. Bidel, S.L. Ustin,  
 1028 G. le Maire, S. Jacquemoud, PROSPECT-4 and 5: Advances in the leaf optical properties  
 1029 model separating photosynthetic pigments, *Remote Sens. Environ.* 112 (2008) 3030–3043.  
 1030 doi:10.1016/j.rse.2008.02.012.

1031 [69] A. Cartelat, Z.G. Cerovic, Y. Goulas, S. Meyer, C. Lelarge, J.L. Prioul, A. Barbottin,  
 1032 M.H. Jeuffroy, P. Gate, G. Agati, I. Moya, Optically assessed contents of leaf  
 1033 polyphenolics and chlorophyll as indicators of nitrogen deficiency in wheat (*Triticum*  
 1034 *aestivum* L.), *F. Crop. Res.* 91 (2005) 35–49. doi:10.1016/j.fcr.2004.05.002.

1035 [70] F. Muchecheti, C. Madakadze, P. Soundy, Leaf chlorophyll readings as an indicator of  
 1036 nitrogen status and yield of spinach (*Spinacia oleracea* L.) grown in soils amended with



1037 Luecaena leucocephala prunings, J. Plant Nutr. 39 (2016) 539–561.  
 1038 doi:10.1080/01904167.2016.1143488.

1039 [71] J. Wang, T. Wang, A.K. Skidmore, T. Shi, G. Wu, Evaluating different methods for grass  
 1040 nutrient estimation from canopy hyperspectral reflectance, Remote Sens. 7 (2015) 5901–  
 1041 5917. doi:10.3390/rs70505901.

1042 [72] S. Jacquemoud, W. Verhoef, F. Baret, C. Bacour, P.J. Zarco-Tejada, G.P. Asner, C.  
 1043 François, S.L. Ustin, PROSPECT+SAIL models: A review of use for vegetation  
 1044 characterization, Remote Sens. Environ. 113 (2009) S56–S66.  
 1045 doi:10.1016/j.rse.2008.01.026.

1046 [73] P.J. Zarco-Tejada, J.C. Pushnik, S. Dobrowski, S.L. Ustin, Steady-state chlorophyll a  
 1047 fluorescence detection from canopy derivative reflectance and double-peak red-edge  
 1048 effects, Remote Sens. Environ. 84 (2003) 283–294. doi:10.1016/S0034-4257(02)00113-X.

1049 [74] J. Huang, C. Wei, Y. Zhang, G.A. Blackburn, X. Wang, C. Wei, J. Wang, Meta-analysis  
 1050 of the detection of plant pigment concentrations using hyperspectral remotely sensed data,  
 1051 PLoS One. 10 (2015) 1–26. doi:10.1371/journal.pone.0137029.

1052 [75] K. Berger, C. Atzberger, M. Danner, G. D’Urso, W. Mauser, F. Vuolo, T. Hank,  
 1053 Evaluation of the PROSAIL model capabilities for future hyperspectral model  
 1054 environments: A review study, Remote Sens. 10 (2018). doi:10.3390/rs10010085.

1055 [76] L.V. Junker, I. Ensminger, Relationship between leaf optical properties, chlorophyll  
 1056 fluorescence and pigment changes in senescing Acer saccharum leaves, Tree Physiol. 36  
 1057 (2016) 694–711. doi:10.1093/treephys/tpv148.

1058 [77] P.J. Curran, Remote Sensing of Foliar Chemistry, Remote Sens. Environ. 278 (1989) 271–  
 1059 278. doi:https://doi.org/10.1016/0034-4257(89)90069-2.

- [78] H.K. Lichtenthaler, C. Buschmann, Chlorophylls and Carotenoids : Measurement and Characterization by UV-VIS, in: Curr. Protoc. Food Anal. Chem., John Wiley & Sons, Inc., 2001. doi:doi.org/10.1002/0471142913.faf0403s01.
- [79] S.L. Ustin, M.E. Schaepman, A.A. Gitelson, S. Jacquemoud, M. Schaepman, G.P. Asner, J.A. Gamon, P. Zarco-Tejada, Retrieval of foliar information about plant pigment systems from high resolution spectroscopy, Remote Sens. Environ. 113 (2009) S67–S77. <http://www.sciencedirect.com/science/article/pii/S0034425709000789>.
- [80] M.A. Cho, A.K. Skidmore, A new technique for extracting the red edge position from hyperspectral data: The linear extrapolation method, Remote Sens. Environ. 101 (2006) 181–193. doi:10.1016/j.rse.2005.12.011.
- [81] I. Filella, J. Peñuelas, The red edge position and shape as indicators of plant chlorophyll content, biomass and hydric status, Int. J. Remote Sens. 15 (1994) 1459–1470. doi:10.1080/01431169408954177.
- [82] M. Juvany, M. Müller, S. Munné-Bosch, Photo-oxidative stress in emerging and senescing leaves: A mirror image, J. Exp. Bot. 64 (2013) 3087–3098. doi:10.1093/jxb/ert174.
- [83] M. Archetti, T.F. Döring, S.B. Hagen, N.M. Hughes, S.R. Leather, D.W. Lee, S. Lev-Yadun, Y. Manetas, H.J. Ougham, P.G. Schaberg, H. Thomas, Unravelling the evolution of autumn colours: an interdisciplinary approach, Trends Ecol. Evol. 24 (2009) 166–173. doi:10.1016/j.tree.2008.10.006.
- [84] B. Demmig-Adams, W.W. Adams, The role of xanthophyll cycle carotenoids in the protection of photosynthesis, Trends Plant Sci. 1 (1996) 21–26. doi:10.1016/S1360-1385(96)80019-7.
- [85] K.K. Niyogi, O. Bjorkman, A.R. Grossman, The roles of specific xanthophylls in

1083 photoprotection, *Proc. Natl. Acad. Sci.* 94 (2002) 14162–14167.  
 1084 doi:10.1073/pnas.94.25.14162.

1085 [86] J.A.J.A. Gamon, J. Peñuelas, C.B.B. Field, J. Penuelas, C.B.B. Field, a Narrow-Waveband  
 1086 Spectral Index That Tracks Diurnal Changes in Photosynthetic Efficiency, *Remote Sens.*  
 1087 *Environ.* 41 (1992) 35–44. doi:10.1016/0034-4257(92)90059-S.

1088 [87] M.F. Garbulsky, J. Peñuelas, J. Gamon, Y. Inoue, I. Filella, The photochemical  
 1089 reflectance index (PRI) and the remote sensing of leaf, canopy and ecosystem radiation  
 1090 use efficiencies. A review and meta-analysis, *Remote Sens. Environ.* 115 (2011) 281–297.  
 1091 doi:10.1016/j.rse.2010.08.023.

1092 [88] C.D. Stylinski, J.A. Gamon, W.C. Oechel, Seasonal patterns of reflectance indices,  
 1093 carotenoid pigments and photosynthesis of evergreen chaparral species, *Oecologia.* 131  
 1094 (2002) 366–374. doi:10.1007/s00442-002-0905-9.

1095 [89] A. Porcar-Castell, J.I. Garcia-Plazaola, C.J. Nichol, P. Kolari, B. Olascoaga, N. Kuusinen,  
 1096 B. Fernández-Marín, M. Pulkkinen, E. Juurola, E. Nikinmaa, Physiology of the seasonal  
 1097 relationship between the photochemical reflectance index and photosynthetic light use  
 1098 efficiency, *Oecologia.* 170 (2012) 313–323. doi:10.1007/s00442-012-2317-9.

1099 [90] M. Mónica Giusti, R.E. Wrolstad, Characterization and Measurement of Anthocyanins by  
 1100 UV-visible Spectroscopy, *Handb. Food Anal. Chem.* 2–2 (2005) 19–31.  
 1101 doi:10.1002/0471709085.ch18.

1102 [91] R. Dogwood, T.S. Feild, D.W. Lee, N.M. Holbrook, Why Leaves Turn Red in Autumn .  
 1103 The Role of Anthocyanins in Senescing Leaves of, 127 (2001) 566–574.  
 1104 doi:10.1104/pp.010063.566.

1105 [92] J.B. Féret, A.A. Gitelson, S.D. Noble, S. Jacquemoud, PROSPECT-D: Towards modeling

leaf optical properties through a complete lifecycle, *Remote Sens. Environ.* 193 (2017) 204–215. doi:10.1016/j.rse.2017.03.004.

[93] A.A. Gitelson, O.B. Chivkunova, M.N. Merzlyak, Nondestructive estimation of anthocyanins and chlorophylls in anthocyanic leaves, *Am. J. Bot.* 96 (2009) 1861–1868. doi:10.3732/ajb.0800395.

[94] J.M. Ourcival, R. Joffre, S. Rambal, Exploring the relationships between reflectance and anatomical and biochemical properties in *Quercus ilex* leaves, *New Phytol.* 143 (1999) 351–364. doi:10.1046/j.1469-8137.1999.00456.x.

[95] E. Baldini, O. Facini, F. Nerozzi, F. Rossi, A. Rotondi, Leaf characteristics and optical properties of different woody species, *Trees*. 12 (1997) 73. doi:10.1007/s004680050124.

[96] S. Foley, B. Rivard, G.A. Sanchez-Azofeifa, J. Calvo, Foliar spectral properties following leaf clipping and implications for handling techniques, *Remote Sens. Environ.* 103 (2006) 265–275. doi:10.1016/j.rse.2005.06.014.

[97] L. Grant, Diffuse and specular characteristics of leaf reflectance, *Remote Sens. Environ.* 22 (1987) 309–322. doi:10.1016/0034-4257(87)90064-2.

[98] S. Jacquemoud, Utilisation de la haute résolution spectrale pour l'étude des couverts végétaux : développement d'un modèle de réflectance spectrale, Université Paris VII, 1992.

[99] D.R. Rossatto, R.M. Kolb, A.C. Franco, Leaf anatomy is associated with the type of growth form in Neotropical savanna plants, *Botanique*. 93 (2015) 507–508. doi:https://doi.org/10.1139/cjb-2015-0001.

[100] E.J. Boren, L. Boschetti, D.M. Johnson, Characterizing the Variability of the Structure Parameter in the PROSPECT Leaf Optical Properties Model, *Remote Sens.* 11 (2019)

1129           1236. doi:10.3390/rs11101236.

1130 [101] S. V. Ollinger, Sources of variability in canopy reflectance and the convergent properties  
1131           of plants, *New Phytol.* 189 (2011) 375–394. doi:10.1111/j.1469-8137.2010.03536.x.

1132 [102] B. Baránková, D. Lazár, J. Nauš, Analysis of the effect of chloroplast arrangement on  
1133           optical properties of green tobacco leaves, *Remote Sens. Environ.* 174 (2016) 181–196.  
1134           doi:10.1016/j.rse.2015.12.011.

1135 [103] Y.T. Hanba, H. Kogami, I. Terashima, The effect of growth irradiance on leaf anatomy  
1136           and photosynthesis in *Acer* species differing in light demand, *Plant, Cell Environ.* 25  
1137           (2002) 1021–1030. doi:10.1046/j.1365-3040.2002.00881.x.

1138 [104] L. Li, Z. Ma, Ü. Niinemets, D. Guo, Three Key Sub-leaf Modules and the Diversity of  
1139           Leaf Designs, *Front. Plant Sci.* 8 (2017) 1–8. doi:10.3389/fpls.2017.01542.

1140 [105] A.K.A.K. Knapp, G.A.G.A. Carter, Variability in leaf optical properties among 26 Species  
1141           From A Broad Range Of Habitats, *Am. J. Bot.* 85 (1998) 940–946. doi:10.2307/2446360.

1142 [106] G.P. Asner, R.E. Martin, Spectral and chemical analysis of tropical forests: Scaling from  
1143           leaf to canopy levels, *Remote Sens. Environ.* 112 (2008) 3958–3970.  
1144           doi:10.1016/j.rse.2008.07.003.

1145 [107] R. Houborg, E. Boegh, Mapping leaf chlorophyll and leaf area index using inverse and  
1146           forward canopy reflectance modeling and SPOT reflectance data, *Remote Sens. Environ.*  
1147           112 (2008) 186–202. doi:10.1016/j.rse.2007.04.012.

1148 [108] C.T. de Wit, *Photosynthesis of leaf canopies*, 1965.

1149 [109] D. Haboudane, J.R. Miller, E. Pattey, P.J. Zarco-Tejada, I.B. Strachan, Hyperspectral  
1150           vegetation indices and novel algorithms for predicting green LAI of crop canopies:  
1151           Modeling and validation in the context of precision agriculture, *Remote Sens. Environ.* 90

1152 (2004) 337–352. doi:10.1016/j.rse.2003.12.013.

1153 [110] T. Ge, F. Sui, L. Bai, C. Tong, N. Sun, Effects of water stress on growth, biomass  
 1154 partitioning, and water-use efficiency in summer maize (*Zea mays* L.) throughout the  
 1155 growth cycle, *Acta Physiol. Plant.* 34 (2012) 1043–1053. doi:10.1007/s11738-011-0901-y.

1156 [111] H.B. Shao, L.Y. Chu, C.A. Jaleel, C.X. Zhao, Water-deficit stress-induced anatomical  
 1157 changes in higher plants, *Comptes Rendus - Biol.* 331 (2008) 215–225.  
 1158 doi:10.1016/j.crvi.2008.01.002.

1159 [112] J.G.P.W. Clevers, L. Kooistra, M.E. Schaepman, Using spectral information from the NIR  
 1160 water absorption features for the retrieval of canopy water content, *Int. J. Appl. Earth Obs.*  
 1161 *Geoinf.* 10 (2008) 388–397. doi:10.1016/j.jag.2008.03.003.

1162 [113] J. Peñuelas, I. Filella, C. Biel, L. Serrano, R. Savé, The reflectance at the 950–970 nm  
 1163 region as an indicator of plant water status, *Int. J. Remote Sens.* 14 (1993) 1887–1905.  
 1164 doi:10.1080/01431169308954010.

1165 [114] D.A. Sims, J.A. Gamon, Estimation of vegetation water content and photosynthetic tissue  
 1166 area from spectral reflectance: A comparison of indices based on liquid water and  
 1167 chlorophyll absorption features, *Remote Sens. Environ.* 84 (2003) 526–537.  
 1168 doi:10.1016/S0034-4257(02)00151-7.

1169 [115] N. Katsoulas, A. Elvanidi, K.P. Ferentinos, M. Kacira, T. Bartzanas, C. Kittas, Crop  
 1170 reflectance monitoring as a tool for water stress detection in greenhouses: A review,  
 1171 *Biosyst. Eng.* 151 (2016) 374–398. doi:10.1016/j.biosystemseng.2016.10.003.

1172 [116] E.J. Emengini, G.A. Blackburn, J.C. Theobald, Detection and discrimination of oil and  
 1173 water deficit-induced stress in maize (*Zea mays* L.) using spectral and thermal responses,  
 1174 *IOSR J. Environ. Sci. Toxicol. Food Technol.* 3 (2013) 53–57.

- 1175 [117] D.C. Percival, J.T.A. Proctor, J.P. Privé, Gas exchange, stem water potential and leaf  
1176 orientation of *Rubus idaeus* L. are influenced by drought stress, *J. Hortic. Sci. Biotechnol.*  
1177 73 (1998) 831–840. doi:10.1080/14620316.1998.11511056.
- 1178 [118] F. Baret, T. Fourty, Estimation of leaf water content and specific leaf weight from  
1179 reflectance and transmittance measurements, *Agronomie*. 17 (2007) 455–464.  
1180 doi:10.1051/agro:19970903.
- 1181 [119] P. Ceccato, S. Flasse, S. Tarantola, S. Jacquemoud, J.M. Grégoire, Detecting vegetation  
1182 leaf water content using reflectance in the optical domain, *Remote Sens. Environ.* 77  
1183 (2001) 22–33. doi:10.1016/S0034-4257(01)00191-2.
- 1184 [120] B. Gao, NDWI—A normalized difference water index for, *Remote Sens. Environ.* 266  
1185 (1996) 257–266. doi:10.1016/S0034-4257(96)00067-3.
- 1186 [121] M.T. Yilmaz, E.R. Hunt, T.J. Jackson, Remote sensing of vegetation water content from  
1187 equivalent water thickness using satellite imagery, *Remote Sens. Environ.* 112 (2008)  
1188 2514–2522. doi:10.1016/j.rse.2007.11.014.
- 1189 [122] Q. Tian, Q. Tong, R. Pu, X. Guo, C. Zhao, Spectroscopic determination of wheat water  
1190 status using 1650–1850 nm spectral absorption features, *Int. J. Remote Sens.* 22 (2001)  
1191 2329–2338. doi:10.1080/01431160118199.
- 1192 [123] C.J. Tucker, Remote sensing of leaf water content in the near infrared, *Remote Sens.*  
1193 *Environ.* 10 (1980) 23–32. doi:10.1016/0034-4257(80)90096-6.
- 1194 [124] D.H. Card, D.L. Peterson, P.A. Matson, J.D. Aber, Prediction of leaf chemistry by the use  
1195 of visible and near infrared reflectance spectroscopy, *Remote Sens. Environ.* 26 (1988)  
1196 123–147. doi:10.1016/0034-4257(88)90092-2.
- 1197 [125] S. Jacquemoud, S.L. Ustin, J. Verdebout, G. Schmuck, G. Andreoli, B. Hosgood,

1198 Estimating leaf biochemistry using the PROSPECT leaf optical properties model, Remote  
1199 Sens. Environ. 56 (1996) 194–202. doi:10.1016/0034-4257(95)00238-3.

1200 [126] M. Asif, Sustainability of timber, wood and bamboo in construction, in: Sustain. Constr.  
1201 Mater., Elsevier, 2009: pp. 31–54. doi:10.1533/9781845695842.31.

1202 [127] Q. Liu, L. Luo, L. Zheng, Lignins: Biosynthesis and biological functions in plants, Int. J.  
1203 Mol. Sci. 19 (2018). doi:10.3390/ijms19020335.

1204 [128] Z. Wang, A.K. Skidmore, T. Wang, R. Darvishzadeh, J. Hearne, Applicability of the  
1205 PROSPECT model for estimating protein and cellulose+lignin in fresh leaves, Remote  
1206 Sens. Environ. 168 (2015) 205–218. doi:10.1016/j.rse.2015.07.007.

1207 [129] P.L. Nagler, Y. Inoue, E.P. Glenn, A.L. Russ, C.S.T. Daughtry, Cellulose absorption  
1208 index (CAI) to quantify mixed soil-plant litter scenes, Remote Sens. Environ. 87 (2003)  
1209 310–325. doi:10.1016/j.rse.2003.06.001.

1210 [130] L. Serrano, J. Peñuelas, S.L. Ustin, Remote sensing of nitrogen and lignin in  
1211 Mediterranean vegetation from AVIRIS data, Remote Sens. Environ. 81 (2002) 355–364.  
1212 doi:10.1016/S0034-4257(02)00011-1.

1213 [131] U.R. Chaudhuri, Fundamentals of Petroleum and Petrochemical Engineering, CRC Press,  
1214 2016. doi:10.1201/b10486.

1215 [132] A.. Adeniyi, J.. Afolabi, Determination of total petroleum hydrocarbons and heavy metals  
1216 in soils within the vicinity of facilities handling refined petroleum products in Lagos  
1217 metropolis, Environ. Int. 28 (2002) 79–82. doi:10.1016/S0160-4120(02)00007-7.

1218 [133] M. Doble, A. Kumar, Petroleum Hydrocarbon Pollution, Biotreat. Ind. Effluents. (2007)  
1219 241–253. doi:10.1016/b978-075067838-4/50025-7.

1220 [134] I. Kisic, S. Mesic, F. Basic, V. Brkic, M. Mesic, G. Durn, Z. Zgorelec, L. Bertovic, The



1221 effect of drilling fluids and crude oil on some chemical characteristics of soil and crops,  
 1222 *Geoderma*. 149 (2009) 209–216. doi:10.1016/j.geoderma.2008.11.041.

1223 [135] R. Brewer, J. Nagashima, M. Kelley, M. Heskett, M. Rigby, Risk-based evaluation of total  
 1224 petroleum hydrocarbons in vapor intrusion studies, *Int. J. Environ. Res. Public Health*. 10  
 1225 (2013) 2441–2467. doi:10.3390/ijerph10062441.

1226 [136] R. Turle, T. Nason, H. Malle, P. Fowlie, Development and implementation of the CCME  
 1227 Reference Method for the Canada-Wide Standard for Petroleum Hydrocarbons (PHC) in  
 1228 soil: A case study, *Anal. Bioanal. Chem.* 387 (2007) 957–964. doi:10.1007/s00216-006-  
 1229 0989-x.

1230 [137] J.M. Baker, The effects of oils on plants, *Environ. Pollut.* 1 (1970) 27–44.  
 1231 doi:10.1016/0013-9327(70)90004-2.

1232 [138] P.C. Nagajyoti, K.D. Lee, T.V.M. Sreekanth, Heavy metals, occurrence and toxicity for  
 1233 plants: A review, *Environ. Chem. Lett.* 8 (2010) 199–216. doi:10.1007/s10311-010-0297-  
 1234 8.

1235 [139] P.H. Rosso, J.C. Pushnik, M. Lay, S.L. Ustin, Reflectance properties and physiological  
 1236 responses of *Salicornia virginica* to heavy metal and petroleum contamination, *Environ.*  
 1237 *Pollut.* 137 (2005) 241–252. doi:10.1016/j.envpol.2005.02.025.

1238 [140] A. Balasubramaniam, P.J. Harvey, Scanning electron microscopic investigations of root  
 1239 structural modifications arising from growth in crude oil-contaminated sand, *Environ. Sci.*  
 1240 *Pollut. Res.* 21 (2014) 12651–12661. doi:10.1007/s11356-014-3138-7.

1241 [141] M. Rusin, J. Gospodarek, A. Nadgórska-Socha, G. Barczyk, Effect of petroleum-derived  
 1242 substances on life history traits of black bean aphid (*Aphis fabae* Scop.) and on the growth  
 1243 and chemical composition of broad bean, *Ecotoxicology*. 26 (2017) 308–319.

doi:10.1007/s10646-017-1764-9.

[142] P. Baruah, R.R. Saikia, P.P. Baruah, S. Deka, Effect of crude oil contamination on the chlorophyll content and morpho-anatomy of *Cyperus brevifolius* (Rottb.) Hassk, *Environ. Sci. Pollut. Res.* 21 (2014) 12530–12538. doi:10.1007/s11356-014-3195-y.

[143] N. Merkl, R. Schultze-Kraft, C. Infante, Phytoremediation in the tropics - Influence of heavy crude oil on root morphological characteristics of graminoids, *Environ. Pollut.* 138 (2005) 86–91. doi:10.1016/j.envpol.2005.02.023.

[144] P. Punwong, Y. Juprasong, P. Traiperm, Effects of an oil spill on the leaf anatomical characteristics of a beach plant (*Terminalia catappa* L.), *Environ. Sci. Pollut. Res.* 24 (2017) 21821–21828. doi:10.1007/s11356-017-9814-7.

[145] M. Shahid, C. Dumat, S. Khalid, E. Schreck, T. Xiong, N.K. Niazi, Foliar heavy metal uptake, toxicity and detoxification in plants: A comparison of foliar and root metal uptake, *J. Hazard. Mater.* 325 (2017) 36–58. doi:10.1016/j.jhazmat.2016.11.063.

[146] L. Zhu, Z. Chen, J. Wang, J. Ding, Y. Yu, J. Li, N. Xiao, L. Jiang, Y. Zheng, G.M. Rimmington, Monitoring plant response to phenanthrene using the red edge of canopy hyperspectral reflectance, *Mar. Pollut. Bull.* 86 (2014) 332–341. doi:10.1016/j.marpolbul.2014.06.046.

[147] M. Khamsehchiyan, A.H. Charkhabi, M. Tajik, Effects of crude oil contamination on geotechnical properties of clayey and sandy soils, *Eng. Geol.* 89 (2007) 220–229. doi:10.1016/j.enggeo.2006.10.009.

[148] A. Klamerus-Iwan, E. Błońska, J. Lasota, A. Kalandyk, P. Waligórski, Influence of Oil Contamination on Physical and Biological Properties of Forest Soil after Chainsaw Use, *Water. Air. Soil Pollut.* 226 (2015). doi:10.1007/s11270-015-2649-2.

- 1267 [149] H. ur R. Athar, S. Ambreen, M. Javed, M. Hina, S. Rasul, Z.U. Zafar, H. Manzoor, C.C.  
 1268 Ogbaga, M. Afzal, F. Al-Qurainy, M. Ashraf, Influence of sub-lethal crude oil  
 1269 concentration on growth, water relations and photosynthetic capacity of maize (*Zea mays*  
 1270 L.) plants, *Environ. Sci. Pollut. Res.* 23 (2016) 18320–18331. doi:10.1007/s11356-016-  
 1271 6976-7.
- 1272 [150] I.A. Ogboghodo, E.K. Iruaga, I.O. Osemwota, J.U. Chokor, An Assessment of the Effects  
 1273 of Crude Oil Pollution on Soil Properties, Germination and Growth of Maize (*Zea Mays*)  
 1274 using Two Crude Types – Forcados Light and Escravos Light, *Environ. Monit. Assess.* 96  
 1275 (2004) 143–152. doi:10.1023/B:EMAS.0000031723.62736.24.
- 1276 [151] Y. Wang, J. Feng, Q. Lin, X. Lyu, X. Wang, G. Wang, Effects of crude oil contamination  
 1277 on soil physical and chemical properties in momoge wetland of China, *Chinese Geogr.*  
 1278 *Sci.* 23 (2013) 708–715. doi:10.1007/s11769-013-0641-6.
- 1279 [152] J. Barceló, C. Poschenrieder, Plant water relations as affected by heavy metal stress: A  
 1280 review, *J. Plant Nutr.* 13 (1990) 1–37. doi:10.1080/01904169009364057.
- 1281 [153] M. Nie, M. Lu, Q. Yang, X. Zhang, M. Xiao, L. Jiang, J. Yang, C. Fang, J. Chen, B. Li,  
 1282 Plants ' use of different nitrogen forms in response to crude oil contamination, 159 (2011)  
 1283 157–163. doi:10.1016/j.envpol.2010.09.013.
- 1284 [154] M. Hawrot-Paw, A. Wijatkowski, M. Mikiciuk, Influence of diesel and biodiesel fuel-  
 1285 contaminated soil on microorganisms , growth and development of plants, *Plant Soil*  
 1286 *Environ.* 61 (2015) 189–194. doi:10.17221/974/2014-PSE.
- 1287 [155] S. Jiao, Z. Liu, Y. Lin, J. Yang, W. Chen, G. Wei, Bacterial communities in oil  
 1288 contaminated soils: Biogeography and co- occurrence patterns occurrence patterns, *Soil*  
 1289 *Biol. Biochem.* 98 (2018) 64–73. doi:10.1016/j.soilbio.2016.04.005.

- 1290 [156] J. Liao, J. Wang, D. Jiang, M.C. Wang, Y. Huang, Long-term oil contamination causes  
1291 similar changes in microbial communities of two distinct soils, *Appl. Microbiol.*  
1292 *Biotechnol.* 99 (2015) 10299–10310. doi:10.1007/s00253-015-6880-y.
- 1293 [157] V. Labud, C. Garcia, T. Hernandez, Effect of hydrocarbon pollution on the microbial  
1294 properties of a sandy and a clay soil, *Chemosphere.* 66 (2007) 1863–1871.  
1295 doi:10.1016/j.chemosphere.2006.08.021.
- 1296 [158] Y. Xie, J. Fan, W. Zhu, E. Amombo, Y. Lou, L. Chen, J. Fu, Effect of Heavy Metals  
1297 Pollution on Soil Microbial Diversity and Bermudagrass Genetic Variation, *Front. Plant*  
1298 *Sci.* 7 (2016) 1–12. doi:10.3389/fpls.2016.00755.
- 1299 [159] X. Fu, Z. Cui, G. Zang, Environmental Science Processes & Impacts extraction processes,  
1300 *Environ. Sci. Process. Impacts.* 16 (2014) 1737–1744. doi:10.1039/c3em00618b.
- 1301 [160] K. Zuofa, P. Loganathan, N.O. Isirimah, Effects of crude oil applications to soil on the  
1302 growth and yield of maize, okro and cassava in Nigeria, *Oil Chem. Pollut.* 4 (1988) 249–  
1303 259. doi:10.1016/S0269-8579(88)80001-7.
- 1304 [161] M.C. Martí, D. Camejo, N. Fernández-García, R. Rellán-Álvarez, S. Marques, F. Sevilla,  
1305 A. Jiménez, Effect of oil refinery sludges on the growth and antioxidant system of alfalfa  
1306 plants, *J. Hazard. Mater.* 171 (2009) 879–885. doi:10.1016/j.jhazmat.2009.06.083.
- 1307 [162] L. Nogueira, C. Inckot, G.D.O. Santos, Phytotoxicity of petroleum-contaminated soil and  
1308 bioremediated soil on *Allophylus edulis*, *Rodriguésia.* 62 (2011) 459–466.
- 1309 [163] A.G. Balliana, B.B. Moura, R.C. Inckot, C. Bona, Development of *Canavalia ensiformis*  
1310 in soil contaminated with diesel oil, *Environ. Sci. Pollut. Res.* 24 (2017) 979–986.  
1311 doi:10.1007/s11356-016-7674-1.
- 1312 [164] J. Dupuy, S. Ouvrard, P. Leglize, T. Sterckeman, Morphological and physiological

- 1313 responses of maize (*Zea mays*) exposed to sand contaminated by phenanthrene,  
1314 Chemosphere. 124 (2015) 110–115. doi:10.1016/j.chemosphere.2014.11.051.
- 1315 [165] I.D. Sanches, C.R. Souza Filho, L.A. Magalhães, G.C.M. Quitério, M.N. Alves, W.J.  
1316 Oliveira, Unravelling remote sensing signatures of plants contaminated with gasoline and  
1317 diesel: An approach using the red edge spectral feature, Environ. Pollut. 174 (2013) 16–  
1318 27. doi:10.1016/j.envpol.2012.10.029.
- 1319 [166] A.K. Shanker, C. Cervantes, H. Loza-Tavera, S. Avudainayagam, Chromium toxicity in  
1320 plants, Environ. Int. 31 (2005) 739–753. doi:10.1016/j.envint.2005.02.003.
- 1321 [167] G.O. Anoliefo, D.E. Vwioko, Effects of spent lubricating oil on the growth of *Capsicum*  
1322 *annuum* L. and *Lycopersicon esculentum* Miller, Environ. Pollut. 88 (1995) 361–364.  
1323 doi:10.1016/0269-7491(95)93451-5.
- 1324 [168] I. Pérez-Hernández, S. Ochoa-Gaona, R.H. Adams, M.C. Rivera-Cruz, V. Pérez-  
1325 Hernández, A. Jarquín-Sánchez, V. Geissen, P. Martínez-Zurimendi, Growth of four  
1326 tropical tree species in petroleum-contaminated soil and effects of crude oil  
1327 contamination, Environ. Sci. Pollut. Res. 24 (2017) 1769–1783. doi:10.1007/s11356-016-  
1328 7877-5.
- 1329 [169] N. Merkl, R. Schultze-Kraft, C. Infante, Phytoremediation in the tropics-the effect of  
1330 crude oil on the growth of tropical plants, Bioremediat. J. 8 (2004) 177–184.  
1331 doi:10.1080/10889860490887527.
- 1332 [170] G. Kvesitadze, G. Khatisashvili, T. Sadunishvili, J.J. Ramsden, Biochemical Mechanisms  
1333 of Detoxification in Higher Plants, Springer-Verlag Berlin Heidelberg, 2006.
- 1334 [171] Y. Li, J.T. Morris, D.C. Yoch, Chronic Low Level Hydrocarbon Amendments Stimulate  
1335 Plant Growth and Microbial Activity in Salt-Marsh Microcosms, J. Appl. Ecol. 27 (1990)

159–171. doi:10.2307/2403575.

[172] G. Lassalle, A. Credo, R. Hédacq, G. Bertoni, D. Dubucq, S. Fabre, A. Elger, Estimating persistent oil contamination in tropical region using vegetation indices and random forest regression, *Ecotoxicol. Environ. Saf.* 184 (2019) 109654. doi:10.1016/j.ecoenv.2019.109654.

[173] N.N. Haroni, Z. Badehian, M. Zarafshar, S. Bazot, The effect of oil sludge contamination on morphological and physiological characteristics of some tree species, *Ecotoxicology*. 28 (2019) 507–519. doi:10.1007/s10646-019-02034-0.

[174] G. Han, B.X. Cui, X.X. Zhang, K.R. Li, The effects of petroleum-contaminated soil on photosynthesis of *Amorpha fruticosa* seedlings, *Int. J. Environ. Sci. Technol.* 13 (2016) 2383–2392. doi:10.1007/s13762-016-1071-7.

[175] C.O. Adenipekun, O.J. Oyetunji, L.S. Kassim, Effect of spent engine oil on the growth parameters and chlorophyll content of *Corchorus olitorius* Linn, *Environmentalist*. 28 (2008) 446–450. doi:10.1007/s10669-008-9165-5.

[176] C. Nakata, C. Qualizza, M. MacKinnon, S. Renault, Growth and physiological responses of *Triticum aestivum* and *Deschampsia caespitosa* exposed to petroleum coke, *Water. Air. Soil Pollut.* 216 (2011) 59–72. doi:10.1007/s11270-010-0514-x.

[177] G. Malallah, M. Afzal, S. Gulshan, D. Abraham, M. Kurian, M.S.I. Dhani, *Vicia faba* as a bioindicator of oil pollution, *Environ. Pollut.* 92 (1996) 213–217. doi:10.1016/0269-7491(95)00085-2.

[178] S.M. De Jong, E.A. Addink, P. Hoogenboom, W. Nijland, The spectral response of *Buxus sempervirens* to different types of environmental stress - A laboratory experiment, *ISPRS J. Photogramm. Remote Sens.* 74 (2012) 56–65. doi:10.1016/j.isprsjprs.2012.08.005.

- 1359 [179] A. Lowe, N. Harrison, A.P. French, Hyperspectral image analysis techniques for the  
1360 detection and classification of the early onset of plant disease and stress, *Plant Methods*.  
1361 13 (2017) 1–12. doi:10.1186/s13007-017-0233-z.
- 1362 [180] K.L. Smith, M.D. Steven, J.J. Colls, Plant spectral responses to gas leaks and other  
1363 stresses, *Int. J. Remote Sens.* 26 (2005) 4067–4081. doi:10.1080/01431160500165625.
- 1364 [181] H.C. Stimson, D.D. Breshears, S.L. Ustin, S.C. Kefauver, Spectral sensing of foliar water  
1365 conditions in two co-occurring conifer species: *Pinus edulis* and *Juniperus monosperma*,  
1366 *Remote Sens. Environ.* 96 (2005) 108–118. doi:10.1016/j.rse.2004.12.007.
- 1367 [182] J.C. Zinnert, S.M. Via, D.R. Young, Distinguishing natural from anthropogenic stress in  
1368 plants: Physiology, fluorescence and hyperspectral reflectance, *Plant Soil.* 366 (2013)  
1369 133–141. doi:10.1007/s11104-012-1414-1.
- 1370 [183] E.J. Emengini, G.A. Blackburn, J.C. Theobald, Discrimination of plant stress caused by  
1371 oil pollution and waterlogging using hyperspectral and thermal remote sensing, *J. Appl.*  
1372 *Remote Sens.* 7 (2013). doi:10.1117/1.jrs.7.073476.
- 1373 [184] J.G.P.W.P.W. Clevers, L. Kooistra, E.A.L.L. Salas, Study of heavy metal contamination  
1374 in river floodplains using the red-edge position in spectroscopic data, *Int. J. Remote Sens.*  
1375 25 (2004) 3883–3895. doi:10.1080/01431160310001654473.
- 1376 [185] T. Shi, H. Liu, J. Wang, Y. Chen, T. Fei, G. Wu, Monitoring arsenic contamination in  
1377 agricultural soils with reflectance spectroscopy of rice plants, *Environ. Sci. Technol.* 48  
1378 (2014) 6264–6272. doi:10.1021/es405361n.
- 1379 [186] S. Huang, S. Chen, D. Wang, C. Zhou, F. van der Meer, Y. Zhang, Hydrocarbon micro-  
1380 seepage detection from airborne hyper-spectral images by plant stress spectra based on the  
1381 PROSPECT model, *Int. J. Appl. Earth Obs. Geoinf.* 74 (2019) 180–190.

doi:10.1016/j.jag.2018.09.012.

[187] E.J. Emengini, F.C. Ezech, N. Chigbu, Comparative Analysis of Spectral Responses of Varied Plant Species to Oil Stress, *Int. J. Sci. Eng. Res.* 4 (2013) 1421–1427.

[188] S. Gürtler, C.R. de Souza Filho, I.D. Sanches, M.N. Alves, W.J. Oliveira, Determination of changes in leaf and canopy spectra of plants grown in soils contaminated with petroleum hydrocarbons, *ISPRS J. Photogramm. Remote Sens.* 146 (2018) 272–288. doi:10.1016/j.isprsjprs.2018.09.011.

[189] L. Zhu, X. Zhao, L. Lai, J. Wang, L. Jiang, J. Ding, N. Liu, Y. Yu, J. Li, N. Xiao, Y. Zheng, G.M. Rimmington, Soil TPH Concentration Estimation Using Vegetation Indices in an Oil Polluted Area of Eastern China, *PLoS One.* 8 (2013). doi:10.1371/journal.pone.0054028.

[190] A. Apan, A. Held, S. Phinn, J. Markley, Detecting sugarcane ‘orange rust’ disease using EO-1 Hyperion hyperspectral imagery, *Int. J. Remote Sens.* 25 (2004) 489–498. doi:10.1080/01431160310001618031.

[191] R. Darvishzadeh, A. Skidmore, M. Schlerf, C. Atzberger, F. Corsi, M. Cho, LAI and chlorophyll estimation for a heterogeneous grassland using hyperspectral measurements, *ISPRS J. Photogramm. Remote Sens.* 63 (2008) 409–426. doi:10.1016/j.isprsjprs.2008.01.001.

[192] T. Rumpf, A.-K. Mahlein, U. Steiner, E.-C. Oerke, H.-W. Dehne, L. Plümer, Early detection and classification of plant diseases with Support Vector Machines based on hyperspectral reflectance, *Comput. Electron. Agric.* 74 (2010) 91–99. doi:10.1016/j.compag.2010.06.009.

[193] C. Axelsson, A.K. Skidmore, M. Schlerf, A. Fauzi, W. Verhoef, Hyperspectral analysis of



1405 mangrove foliar chemistry using PLSR and support vector regression, *Int. J. Remote Sens.*  
1406 34 (2013) 1724–1743. doi:10.1080/01431161.2012.725958.

1407 [194] T. Hermosilla, M.A. Wulder, J.C. White, N.C. Coops, G.W. Hobart, Regional detection,  
1408 characterization, and attribution of annual forest change from 1984 to 2012 using Landsat-  
1409 derived time-series metrics, *Remote Sens. Environ.* 170 (2015) 121–132.  
1410 doi:10.1016/j.rse.2015.09.004.

1411 [195] R.A. Schowengerdt, *Remote sensing: Models and methods for image processing*, 3rd Ed.,  
1412 Elsevier Inc., 2006. doi:10.1016/C2009-0-21902-7.

1413 [196] M. Story, R.G. Congalton, *Remote Sensing Brief Accuracy Assessment: A User's*  
1414 *Perspective*, *Photogramm. Eng. Remote Sensing*. 52 (1986) 397–399.

1415 [197] M. Belgiu, L. Drăguț, Random forest in remote sensing: A review of applications and  
1416 future directions, *ISPRS J. Photogramm. Remote Sens.* 114 (2016) 24–31.  
1417 doi:10.1016/j.isprsjprs.2016.01.011.

1418 [198] D. Tuia, J. Verrelst, L. Alonso, F. Perez-Cruz, G. Camps-Valls, Multioutput support  
1419 vector regression for remote sensing biophysical parameter estimation, *IEEE Geosci.*  
1420 *Remote Sens. Lett.* 8 (2011) 804–808. doi:10.1109/LGRS.2011.2109934.

1421 [199] F. Melgani, L. Bruzzone, Classification of hyperspectral remote sensing images with  
1422 support vector machines, *IEEE Trans. Geosci. Remote Sens.* 42 (2004) 1778–1790.  
1423 doi:10.1109/TGRS.2004.831865.

1424 [200] G. Hughes, On the mean accuracy of statistical pattern recognizers, *IEEE Trans. Inf.*  
1425 *Theory*. 14 (1968) 55–63. doi:10.1109/TIT.1968.1054102.

1426 [201] P.S. Thenkabail, E.A. Enclona, M.S. Ashton, B. Van Der Meer, Accuracy assessments of  
1427 hyperspectral waveband performance for vegetation analysis applications, *Remote Sens.*

1428 Environ. 91 (2004) 354–376. doi:10.1016/j.rse.2004.03.013.

1429 [202] C. Wei, J. Huang, X. Wang, G.A. Blackburn, Y. Zhang, S. Wang, L.R. Mansaray,  
 1430 Hyperspectral characterization of freezing injury and its biochemical impacts in oilseed  
 1431 rape leaves, Remote Sens. Environ. 195 (2017) 56–66. doi:10.1016/j.rse.2017.03.042.

1432 [203] J.H. Friedman, B.E. Popescu, Gradient Directed Regularization for Linear Regression and  
 1433 Classification, 2004. stanford.

1434 [204] R.A. Fisher, The use of multiple measurements in taxonomic problems, Ann. Eugen. 7  
 1435 (1936) 179–188. doi:10.1111/j.1469-1809.1936.tb02137.x.

1436 [205] D.A. Belsley, E. Kuh, R.E. Wemisch, Detecting and Assessing Collinearity, in: I. John  
 1437 Wiley & Sons (Ed.), Regres. Diagnostics Identifying Influential Data Sources Collinearity,  
 1438 1980.

1439 [206] H. Zou, T. Hastie, Regression and variable selection via the elastic net, J. R. Stat. Soc. Ser.  
 1440 B (Statistical Methodol. 67 (2005) 301–320. doi:10.1111/j.1467-9868.2005.00503.x.

1441 [207] T.Z. Keith, Multiple Regression and Beyond, 2nd Ed., Routledge, 2014.  
 1442 doi:10.4324/9781315749099.

1443 [208] G. Mountrakis, J. Im, C. Ogole, Support vector machines in remote sensing: A review,  
 1444 ISPRS J. Photogramm. Remote Sens. 66 (2011) 247–259.  
 1445 doi:10.1016/j.isprsjprs.2010.11.001.

1446 [209] S. Jacquemoud, S.L. Ustin, Leaf optical properties: A state of the art, 2001.

1447 [210] J. Jiang, A. Comar, P. Burger, P. Bancal, M. Weiss, F. Baret, Estimation of leaf traits from  
 1448 reflectance measurements: comparison between methods based on vegetation indices and  
 1449 several versions of the PROSPECT model, Plant Methods. 14 (2018).  
 1450 doi:10.1186/s13007-018-0291-x.

- 1451 [211] K.M. Barry, G.J. Newnham, C. Stone, Estimation of chlorophyll content in Eucalyptus  
1452 globulus foliage with the leaf reflectance model PROSPECT, *Agric. For. Meteorol.* 149  
1453 (2009) 1209–1213. doi:10.1016/j.agrformet.2009.01.005.
- 1454 [212] B. Adamu, K. Tansey, B. Ogutu, Remote sensing for detection and monitoring of  
1455 vegetation affected by oil spills, *Int. J. Remote Sens.* 39 (2018) 3628–3645.  
1456 doi:10.1080/01431161.2018.1448483.
- 1457 [213] M.S. Ozigis, J.D. Kaduk, C.H. Jarvis, Mapping terrestrial oil spill impact using machine  
1458 learning random forest and Landsat 8 OLI imagery: a case site within the Niger Delta  
1459 region of Nigeria, *Environ. Sci. Pollut. Res.* 26 (2019) 3621–3635. doi:10.1007/s11356-  
1460 018-3824-y.
- 1461 [214] M. van der Meijde, H.M.A. van der Werff, P.F. Jansma, F.D. van der Meer, G.J.  
1462 Groothuis, A spectral-geophysical approach for detecting pipeline leakage, *Int. J. Appl.*  
1463 *Earth Obs. Geoinf.* 11 (2009) 77–82. doi:10.1016/j.jag.2008.08.002.
- 1464 [215] N.N. Onyia, H. Balzter, J.C. Berrio, Detecting vegetation response to oil pollution using  
1465 hyperspectral indices, *Int. Geosci. Remote Sens. Symp.* 2018-July (2018) 3963–3966.  
1466 doi:10.1109/IGARSS.2018.8519398.
- 1467 [216] B. Adamu, K. Tansey, B. Ogutu, An investigation into the factors influencing the  
1468 detectability of oil spills using spectral indices in an oil-polluted environment, *Int. J.*  
1469 *Remote Sens.* 37 (2016) 2338–2357. doi:10.1080/01431161.2016.1176271.
- 1470 [217] F. Salem, M. Kafatos, T. El-Ghazawi, R. Gomez, R. Yang, Hyperspectral image  
1471 assessment of oil-contaminated wetland, *Int. J. Remote Sens.* 26 (2005) 811–821.  
1472 doi:10.1080/01431160512331316883.
- 1473 [218] M.H. Tangestani, K. Validabadi, Mineralogy and geochemistry of alteration induced by

hydrocarbon seepage in an evaporite formation; a case study from the Zagros Fold Belt, SW Iran, *Appl. Geochemistry*. 41 (2014) 189–195. doi:10.1016/j.apgeochem.2013.12.015.

[219] I. Leifer, W.J. Lehr, D. Simecek-Beatty, E. Bradley, R. Clark, P. Dennison, Y. Hu, S. Matheson, C.E. Jones, B. Holt, M. Reif, D.A. Roberts, J. Svejksky, G. Swayze, J. Wozencraft, State of the art satellite and airborne marine oil spill remote sensing: Application to the BP Deepwater Horizon oil spill, *Remote Sens. Environ.* 124 (2012) 185–209. doi:10.1016/J.RSE.2012.03.024.

[220] P. Arellano, K. Tansey, H. Balzter, M. Tellkamp, Plant family-specific impacts of petroleum pollution on biodiversity and leaf chlorophyll content in the Amazon rainforest of Ecuador, *PLoS One*. 12 (2017). doi:10.1371/journal.pone.0169867.

[221] Y. Zhong, L. Zhao, L. Zhang, An adaptive differential evolution endmember extraction algorithm for hyperspectral remote sensing imagery, *IEEE Geosci. Remote Sens. Lett.* 11 (2014) 1061–1065. doi:10.1109/LGRS.2013.2285476.

[222] S. Stagakis, T. Vanikiotis, O. Sykioti, Estimating forest species abundance through linear unmixing of CHRIS/PROBA imagery, *ISPRS J. Photogramm. Remote Sens.* 119 (2016) 79–89. doi:10.1016/j.isprsjprs.2016.05.013.

[223] R. Dehaan, J. Louis, A. Wilson, A. Hall, R. Rumbachs, Discrimination of blackberry (*Rubus fruticosus* sp. agg.) using hyperspectral imagery in Kosciuszko National Park, NSW, Australia, *ISPRS J. Photogramm. Remote Sens.* 62 (2007) 13–24. doi:10.1016/j.isprsjprs.2007.01.004.

[224] I. Colomina, P. Molina, Unmanned aerial systems for photogrammetry and remote sensing: A review, *ISPRS J. Photogramm. Remote Sens.* 92 (2014) 79–97. doi:10.1016/j.isprsjprs.2014.02.013.

- 1497 [225] B. Lu, Y. He, Species classification using Unmanned Aerial Vehicle (UAV)-acquired high  
1498 spatial resolution imagery in a heterogeneous grassland, *ISPRS J. Photogramm. Remote*  
1499 *Sens.* 128 (2017) 73–85. doi:10.1016/j.isprsjprs.2017.03.011.
- 1500 [226] M.A. Wulder, J.C. White, R.F. Nelson, E. Næsset, H.O. Ørka, N.C. Coops, T. Hilker,  
1501 C.W. Bater, T. Gobakken, Lidar sampling for large-area forest characterization: A review,  
1502 *Remote Sens. Environ.* 121 (2012) 196–209. doi:10.1016/j.rse.2012.02.001.
- 1503 [227] M.S. Ozgis, J.D. Kaduk, C.H. Jarvis, P. da Conceição Bispo, H. Balzter, Detection of oil  
1504 pollution impacts on vegetation using multifrequency SAR, multispectral images with  
1505 fuzzy forest and random forest methods, *Environ. Pollut.* (2019).  
1506 doi:10.1016/j.envpol.2019.113360.
- 1507 [228] Yi Hyun Kim, T. Jackson, R. Bindlish, Hoonyol Lee, Sukyoung Hong, Radar Vegetation  
1508 Index for Estimating the Vegetation Water Content of Rice and Soybean, *IEEE Geosci.*  
1509 *Remote Sens. Lett.* 9 (2012) 564–568. doi:10.1109/LGRS.2011.2174772.
- 1510